

Complexity Guarantees for Nonconvex Newton-MR Under Inexact Hessian Information

Alexander Lim* Fred Roosta†

August 22, 2023

Abstract

We consider extensions of the Newton-MR algorithm for nonconvex optimization, proposed in [43], to the settings where Hessian information is approximated. Under additive noise model on the Hessian matrix, we investigate the iteration and operation complexities of these variants to achieve first and second-order sub-optimality criteria. We show that, under certain conditions, the algorithms achieve iteration and operation complexities that match those of the exact variant. Focusing on the particular nonconvex problems satisfying Polyak-Lojasiewicz condition, we show that our algorithm achieves a linear convergence rate. We finally compare the performance of our algorithms with several alternatives on a few machine learning problems.

1 Introduction

We consider the following unconstrained optimization problem:

$$\min_{\mathbf{x} \in \mathbb{R}^d} f(\mathbf{x}), \quad (1)$$

where $f : \mathbb{R}^d \rightarrow \mathbb{R}$ is twice continuously differentiable and nonconvex. Among all possible methods for solving (1) are the class of first-order algorithms [2, 37, 39] and those exploiting some form of curvature information, i.e. second-order methods [20, 46]. Among these latter class of algorithms are methods with globalization strategies based on trust region [23, 62] and cubic regularization [18, 19, 45, 62], as well as those employing line-search such as variants of the classical Newton-CG [53, 65], methods based on conjugate residual [24], and more recently Newton-MR variants [41, 43, 51], which rely on minimum residual (MINRES) sub-problem solver.

Arguably, operations involving the Hessian matrix, such as matrix-vector products, are often the primary source of computational costs in second-order algorithms. For example, for large-scale finite sum minimization problems [56, 63] where $f(\mathbf{x}) = \sum_{i=1}^n f_i(\mathbf{x})/n$ and $n \gg 1$, such operations typically constitute the main bottleneck of computations. To address this computational burden, the focus lies in designing algorithms that utilize appropriate approximations of the Hessian matrix while preserving much of the desirable convergence behavior of the original exact methods. This area of research has gained significant attention in recent years, leading to the development of different variants of second-order methods that incorporate various forms of Hessian approximations; see the related work below.

Focusing on second-order methods with line-search globalization strategies, however, almost all such efforts have centered around Newton-type algorithms that employ the conjugate gradient algorithm as their respective sub-problem solver, e.g., variants of Newton-CG [3, 8, 14, 52, 66]. One exception can be found in [41] where the Newton-MR algorithm, initially proposed in [51], is extended to incorporate Hessian approximation. Unlike Newton-CG, the Newton-MR framework relies on MINRES [42, 48] as the sub-problem solver. However, the Newton-MR variants discussed in [41, 51] are limited in their scope to invex problems [44]. To overcome this limitation, recently [43] proposes a novel variant of Newton-MR that, by employing nonpositive curvature directions arising as part of the MINRES iterations, can be readily applied to more general nonconvex settings. Here, we aim to extend this algorithm to accommodate inexact Hessian information, while ensuring that it maintains similar convergence complexities as the original method.

*School of Mathematics and Physics, University of Queensland, Australia. Email : alexander.lim@uq.edu.au

†School of Mathematics and Physics, and ARC Training Centre for Information Resilience, University of Queensland, Australia. Email : fred.roosta@uq.edu.au

The rest of this paper is organized as follows. We end this section by briefly reviewing the related work, followed by presenting the essential notations and definitions used in this paper, as well as our contributions. In Section 2, we review the algorithms and conditions, which are initially introduced in [42, 43]. In Section 3, we begin our theoretical analyses. To set the scene, in Section 3.1 we present convergence analysis of our algorithm for a very special class of nonconvex functions, namely those satisfying the Polyak-Lojasiewicz assumption. We then proceed to general nonconvex settings in Section 3.2. First and second-order complexity analyses are given, respectively, in Sections 3.2.1 and 3.2.2. In Section 4, we evaluate the performance of our algorithms on several machine learning problems. Conclusions and further thoughts are gathered in Section 5.

Related Work

Since the advent of deep learning and neural networks, there have been studies of numerical optimization algorithms from the perspective of machine learning. In particular, the first-order algorithms, like gradient descent and such, have been widely used in the machine learning and data analysis research [1, 29, 37, 39, 55, 59, 61]. While first-order algorithms enjoy from being memory efficient, low-cost per iteration and simple to implement, they are also notoriously difficult to fine tune and slow in convergence, especially when the functions are not well-conditioned. On the other hand, there are second-order algorithms, like Newton’s method [23, 46, 53, 66, 67, 68], L-BFGS [40], and cubic regularization [4, 5, 7, 17, 18, 19, 45], which incorporate second-order information. Many of these algorithms have the ability to efficiently escape saddle points, low gradient regions and achieve second-order optimality. Apart from the commonly known advantages, it is also empirically shown to be less sensitive to hyper-parameters tuning, arguably resulting in total computational time being less than the ones in first-order methods [10, 63].

To accommodate the fast growing data era, extensive studies have been done in using inexact functions approximation. This allows for reduction in both computational memory and time, but still maintaining the overall convergence rate. For example, inexact Hessian [17, 18, 19, 41, 62] and/or inexact gradient [4, 5, 60, 65, 66] are used in different algorithms. In some studies, the approximation even extends to the objective function itself [6, 13, 21, 22, 33, 38, 57]. Furthermore, there are also recent rise of interests in OFFO methods, Objective Function Free Optimization, to dispense of the evaluation of the objective function [31, 32, 34].

In finite-sum settings, the approximation of Hessian is typically done through random sub-sampling [5, 7, 9, 10, 11, 14, 15, 16, 27, 41, 52]. In certain special cases, the structure of f could also be used for more sophisticated randomized matrix approximation strategies such as sketching and those based on statistical leverage scores, e.g., [50, 64].

Notations and Definitions

Throughout the paper, vectors and matrices are, respectively, denoted by bold lower and upper case letters, e.g. \mathbf{a} and \mathbf{A} . Their respective norms, e.g., $\|\mathbf{a}\|$ and $\|\mathbf{A}\|$, are Euclidean and matrix spectral norms. Regular letters represent scalar constants, e.g. d, L, n , etc. We denote the exact and the inexact Hessian as \mathbf{H} and $\bar{\mathbf{H}}$, respectively. We use subscripts to denote the iteration counter of our algorithms, e.g., \mathbf{x}_k . The objective function and its gradient at iteration k are denoted by $f_k \triangleq f(\mathbf{x}_k)$ and $\mathbf{g}_k \triangleq \mathbf{g}(\mathbf{x}_k)$, respectively. We use superscripts to denote the iterations of MINRES. Specifically, $\mathbf{p}_k^{(t)}$ refers to the t^{th} iteration of MINRES using $\bar{\mathbf{H}}_k$ and \mathbf{g}_k with the corresponding residual $\mathbf{r}_k^{(t)} = -\bar{\mathbf{H}}_k \mathbf{p}_k^{(t)} - \mathbf{g}_k$. The Krylov subspace of degree t , generated by $\bar{\mathbf{H}}_k$ and \mathbf{g}_k , is denoted by $\mathcal{K}_t(\bar{\mathbf{H}}_k, \mathbf{g}_k)$. Natural logarithm is denoted $\log(\cdot)$. Logarithmic factors in the ‘big-O’ notation are indicated by $\tilde{O}(\cdot)$. We also denote $f^* \triangleq \min f(\mathbf{x})$. In all of our analysis, the eigenvalues are ordered from largest to smallest, i.e., we index a given set of eigenvalues as $\lambda_1 \geq \lambda_2 \geq \dots \geq \lambda_d$.

In nonconvex settings, one’s objective is often to find solutions that satisfy a certain level of approximate local optimality. In this paper, we adopt the following widely used notion of approximate optimality.

Definition 1 ($(\varepsilon_{\mathbf{g}}, \varepsilon_{\mathbf{H}})$ -Optimality). *Given $0 < \varepsilon_{\mathbf{g}} < 1$ and $0 < \varepsilon_{\mathbf{H}} < 1$, a point $\mathbf{x} \in \mathbb{R}^d$ is an $(\varepsilon_{\mathbf{g}}, \varepsilon_{\mathbf{H}})$ -optimal solution to the problem (1) if*

$$\|\mathbf{g}(\mathbf{x})\| \leq \varepsilon_{\mathbf{g}}, \tag{2a}$$

$$\lambda_{\min}(\mathbf{H}(\mathbf{x})) \geq -\varepsilon_{\mathbf{H}}. \tag{2b}$$

For a point \mathbf{x} , if both (2a) and (2b) hold, it is said to satisfy second-order sub-optimality condition. However, if \mathbf{x} only satisfies (2a), it is referred to as a first-order sub-optimal point.

The geometry of the optimization landscape is essentially encoded in the spectrum of the Hessian matrix. In and around saddle regions, where the gradient is unreliably small (or even zero), one can obtain descent by leveraging directions that, to a great degree, align with the eigenspace associated with the nonpositive eigenvalues of the Hessian. These directions are referred to as nonpositive curvature (NPC) directions.

Definition 2 (Nonpositive Curvature direction). For any non-zero $\mathbf{x} \in \mathbb{R}^d$, we call \mathbf{x} a nonpositive curvature (NPC) direction for a matrix \mathbf{A} , if

$$\langle \mathbf{x}, \mathbf{A}\mathbf{x} \rangle \leq 0.$$

Contribution

In this paper, we design and analyze inexact variants of nonconvex Newton-MR, initially proposed in [43], where the Hessian is approximated (Algorithms 4 and 5). We consider an additive noise model to the Hessian matrix, that is,

$$\bar{\mathbf{H}}(\mathbf{x}) = \mathbf{H}(\mathbf{x}) + \mathbf{E}(\mathbf{x}), \quad (3a)$$

where $\mathbf{E}(\mathbf{x})$ is some symmetric noise matrix, potentially depending on \mathbf{x} , such that for some $\varepsilon > 0$,

$$\|\mathbf{E}(x)\| \leq \varepsilon. \quad (3b)$$

We show that our algorithms maintain the convergence and complexity properties of the original exact algorithm from [43]. Specifically, to achieve $(\varepsilon_{\mathbf{g}}, \varepsilon_{\mathbf{H}})$ -optimality (Definition 1), under certain assumptions, we show the following.

Results and Contributions (Informal)

1. By leveraging the properties of MINRES, we first show that, under mild assumptions and more notably for *any* ε , our simple algorithm (Algorithm 4) can achieve linear convergence rate for functions with Polyak-Łojasiewicz property (Theorem 1).
2. We then consider more general nonconvex settings and through a fine-grained analysis, show that our algorithm (Algorithm 4) achieves the *optimal* first-order iteration and operation complexities of $\mathcal{O}(\varepsilon_{\mathbf{g}}^{-3/2})$ (Theorem 2) and $\tilde{\mathcal{O}}(\varepsilon_{\mathbf{g}}^{-3/2})$ (Theorem 3), respectively.
3. We also show that an extension of our algorithm (Algorithm 5) achieves the *optimal* second-order iteration complexity of $\max\left\{\mathcal{O}(\varepsilon_{\mathbf{H}}^{-3}), \mathcal{O}(\varepsilon_{\mathbf{g}}^{-3/2})\right\}$ (Theorem 4) and the *state-of-the-art* operation complexity of $\max\left\{\tilde{\mathcal{O}}(\varepsilon_{\mathbf{H}}^{-7/2}), \tilde{\mathcal{O}}(\varepsilon_{\mathbf{g}}^{-3/2})\right\}$ (Theorem 5), respectively.
4. We provide numerical examples that showcase the advantages of our algorithms for some machine learning problems.

2 Newton-MR with Inexact Hessian

We now present our variants of Newton-MR that incorporates inexact Hessian information. As compared with the original algorithms in [43], the modifications are straightforward: we simply replace all appearance of the exact Hessian matrix, \mathbf{H} , with an approximation, $\bar{\mathbf{H}}$. The core of our algorithms lies on MINRES, depicted in Algorithm 1, as the sub-problem solver. Recall that the t^{th} iterate of Algorithm 1 is given as

$$\mathbf{s}_k^{(t)} = \arg \min_{\mathbf{s} \in \mathcal{K}_t(\bar{\mathbf{H}}_k, \mathbf{g}_k)} \|\bar{\mathbf{H}}_k \mathbf{s} + \mathbf{g}_k\|^2,$$

Algorithm 1 MINRES($\bar{\mathbf{H}}, \mathbf{g}, \eta$) (see [42] for more detailed discussion on MINRES)

Require: Inexact Hessian $\bar{\mathbf{H}}$, Gradient \mathbf{g} , Inexactness tolerance $\eta > 0$

```

1:  $\phi_0 = \tilde{\beta}_1 = \|\mathbf{g}\|$ ,  $\mathbf{r}_0 = -\mathbf{g}$ ,  $\mathbf{v}_1 = \mathbf{r}_0/\phi_0$ ,  $\mathbf{v}_0 = \mathbf{s}_0 = \mathbf{w}_0 = \mathbf{w}_{-1} = \mathbf{0}$ ,
2:  $c_0 = -1$ ,  $\delta_1^{(1)} = s_0 = \tau_0 = 0$ , Type = SOL,
3:  $t = 1$ 
4: while True do
5:    $\mathbf{q}_t = \bar{\mathbf{H}}\mathbf{v}_t$ ,  $\tilde{\alpha}_t = \mathbf{v}_t^\top \mathbf{q}_t$ ,  $\mathbf{q}_t = \mathbf{q}_t - \tilde{\beta}_t \mathbf{v}_{t-1} - \tilde{\alpha}_t \mathbf{v}_t$ ,  $\tilde{\beta}_{t+1} = \|\mathbf{q}_t\|$ 
6:    $\begin{bmatrix} \delta_t^{(2)} & \epsilon_{t+1} \\ \gamma_t^{(1)} & \delta_{t+1}^{(1)} \end{bmatrix} = \begin{bmatrix} c_{t-1} & s_{t-1} \\ s_{t-1} & -c_{t-1} \end{bmatrix} \begin{bmatrix} \delta_t^{(1)} & 0 \\ \tilde{\alpha}_t & \tilde{\beta}_{t+1} \end{bmatrix}$ 
7:   if  $\phi_{t-1} \sqrt{[\gamma_t^{(1)}]^2 + [\delta_{t+1}^{(1)}]^2} \leq \eta \sqrt{\phi_0^2 - \phi_{t-1}^2}$  then
8:     Type = SOL
9:     return  $\mathbf{s}_{t-1}$ , Type
10:  end if
11:  if  $c_{t-1} \gamma_t^{(1)} \geq 0$  then
12:    Type = NPC
13:    return  $\mathbf{r}_{t-1}$ , Type
14:  end if
15:   $\gamma_t^{(2)} = \sqrt{[\gamma_t^{(1)}]^2 + \tilde{\beta}_{t+1}^2}$ 
16:  if  $\gamma_t^{(2)} \neq 0$  then
17:     $c_t = \gamma_t^{(1)}/\gamma_t^{(2)}$ ,  $s_t = \tilde{\beta}_{t+1}/\gamma_t^{(2)}$ ,  $\tau_t = c_t \phi_{t-1}$ ,  $\phi_t = s_t \phi_{t-1}$ ,
18:     $\mathbf{w}_t = (\mathbf{v}_t - \delta_t^{(2)} \mathbf{w}_{t-1} - \epsilon_t^{(1)} \mathbf{w}_{t-2}) / \gamma_t^{(2)}$ ,  $\mathbf{s}_t = \mathbf{s}_{t-1} + \tau_t \mathbf{w}_t$ 
19:    if  $\tilde{\beta}_{t+1} \neq 0$  then
20:       $\mathbf{v}_{t+1} = \mathbf{q}_t / \tilde{\beta}_{t+1}$ ,  $\mathbf{r}_t = s_t^2 \mathbf{r}_{t-1} - \phi_t c_t \mathbf{v}_{t+1}$ 
21:    end if
22:  else
23:     $c_t = 0$ ,  $s_t = 1$ ,  $\tau_t = 0$ ,  $\phi_t = \phi_{t-1}$ ,  $\mathbf{r}_t = \mathbf{r}_{t-1}$ ,  $\mathbf{s}_t = \mathbf{s}_{t-1}$ 
24:  end if  $t = t + 1$ 
25: end while
26: return  $\mathbf{x}_t$ 

```

where we have used the notation $\mathbf{s}_k^{(t)}$ to refer to the MINRES iterate \mathbf{s}_t obtained at iteration t from $\bar{\mathbf{H}}_k$ and \mathbf{g}_k . It has been shown that Algorithm 1 enjoys several desirable monotonicity properties as well as an inherent ability to detect directions of nonpositive curvature [42]. These properties are leveraged within Newton-MR framework to obtain algorithms that can be readily applied to many nonconvex problems.

At every iteration of MINRES within our algorithms, two criteria are checked, namely *sub-problem inexactness condition* and *NPC condition*. It turns out that of both these conditions can be readily verified as part of the MINRES iterations by simple scalar multiplications and without any additional vector operations or matrix-vector products. However, at a given MINRES iteration, some of the underlying scalars are only available at the beginning of the next iterations, and hence the conditions are given in terms of iteration $t - 1$; see [43] for details.

Condition 1 (Sub-problem Inexactness Condition). *At iteration t of MINRES, if*

$$\left\| \bar{\mathbf{H}}_k \mathbf{r}_k^{(t-1)} \right\| < \eta \left\| \bar{\mathbf{H}}_k \mathbf{s}_k^{(t-1)} \right\|,$$

then $\mathbf{s}_k^{(t-1)}$ is declared as a solution direction satisfying the sub-problem inexactness condition where $\eta > 0$ is any given inexactness parameter and $\mathbf{r}_k^{(t-1)} = -\bar{\mathbf{H}}_k \mathbf{s}_k^{(t-1)} - \mathbf{g}_k$. This condition is effortlessly verified in Step 7 of Algorithm 1.

We emphasize that Condition 1 is guaranteed to be eventually satisfied during the iterations [43], regardless of the choice of η . This is in sharp contrast to the typical relative residual condition, $\left\| \mathbf{r}_k^{(t-1)} \right\| \leq \eta \|\mathbf{g}_k\|$, often used in related works. In nonconvex settings, where the gradient might not lie entirely in the range of Hessian, the relative residual condition might never be satisfied unless the inexactness parameter is appropriately set, which itself depends on some unavailable lower-bound; see [43] for more discussion on this choice of sub-problem inexactness condition.

Condition 2 (NPC Condition). *At iteration t of MINRES, if*

$$\left\langle \mathbf{r}_k^{(t-1)}, \bar{\mathbf{H}}_k \mathbf{r}_k^{(t-1)} \right\rangle \leq 0,$$

then $\mathbf{r}_k^{(t-1)}$ is declared as an NPC direction, where $\mathbf{r}_k^{(t-1)} = -\bar{\mathbf{H}}_k \mathbf{s}_k^{(t-1)} - \mathbf{g}_k$. This condition is effortlessly verified in Step 11 of Algorithm 1.

It can be shown that one of Conditions 1 and 2 is guaranteed to be eventually satisfied [42, 43]. In this light, the search direction for our algorithm is constructed as follows:

$$\mathbf{d}_k = \begin{cases} \mathbf{s}_k^{(t-1)}, & \text{(if Condition 1 is satisfied),} \\ \mathbf{r}_k^{(t-1)}, & \text{(if Condition 2 is satisfied).} \end{cases}$$

As long as no NPC direction has been detected, one can show that $\langle \mathbf{s}_k^{(t-1)}, \mathbf{g}_k \rangle < 0$. In fact, for the NPC direction also, we are always guaranteed to have $\langle \mathbf{r}_k^{(t-1)}, \mathbf{g}_k \rangle < 0$. As a result, the search direction \mathbf{d}_k generated from MINRES is always guaranteed to yield descent for f . To yield sufficient descents for each iteration, we enforce a step size α_k satisfying Armijo-type line-search,

$$f(\mathbf{x}_k + \alpha_k \mathbf{d}_k) \leq f(\mathbf{x}_k) + \rho \alpha_k \langle \mathbf{g}_k, \mathbf{p}_k \rangle \quad (4)$$

In particular, when $\mathbf{d}_k = \mathbf{s}_k^{(t-1)}$, we perform Algorithm 2 with $\rho = \rho_S$ where $0 < \rho_S < 1/2$ to obtain the largest $0 < \alpha_k \leq 1$. When $\mathbf{d}_k = \mathbf{r}_k^{(t-1)}$, we perform Algorithm 3 with $\rho = \rho_N$ where $0 < \rho_N < 1$ to obtain the largest $0 < \alpha_k < \infty$. After a step size, α_k is found, the next iterate is then given as $\mathbf{x}_{k+1} = \mathbf{x}_k + \alpha_k \mathbf{d}_k$. The simplest variant of our Newton-MR variant incorporating inexact Hessian is depicted in Algorithm 4. One can see that Algorithm 4 is almost identical to its counterpart in [43], with the exception that, instead of \mathbf{H} , we use its approximation $\bar{\mathbf{H}}$.

For the sake of brevity, we have introduced a variable “Type” in Algorithm 4 and in our subsequent discussions. This variable takes the value “Type = SOL” when Condition 1 is triggered, indicating $\mathbf{d}_k = \mathbf{s}_k^{(t-1)}$, and it is set to “Type = NPC” when Condition 2 is met, signifying $\mathbf{d}_k = \mathbf{r}_k^{(t-1)}$.

Algorithm 2 Backward Tracking Line-Search [43]

Require: $\alpha = 1, 0 < h < 1$

- 1: **while** (4) is not satisfied **do**
 - 2: $\alpha = h\alpha$
 - 3: **end while**
 - 4: **return** α
-

Algorithm 3 Forward/Backward Tracking Line-Search [43]

Require: $\alpha > 0, 0 < h < 1$

- 1: **if** (4) is not satisfied **then**
 - 2: Call Algorithm 2
 - 3: **else**
 - 4: **while** (4) is satisfied **do**
 - 5: $\alpha = \alpha/h$
 - 6: **end while**
 - 7: **return** $h\alpha$
 - 8: **end if**
-

Algorithm 4 Newton-MR with Inexact Hessian

Require:

- Initial point: \mathbf{x}_0
- First-order optimality tolerance: $0 < \varepsilon_{\mathbf{g}} \leq 1$
- Sub-problem Inexactness tolerance : $\eta > 0$

- 1: $k = 0$
 - 2: **while** $\|\mathbf{g}_k\| > \varepsilon_{\mathbf{g}}$ **do**
 - 3: Call MINRES Algorithm 1: $(\mathbf{d}_k, \text{Type}) = \text{MINRES}(\bar{\mathbf{H}}_k, \mathbf{g}_k, \eta)$
 - 4: **if** $\text{Type} = \text{SOL}$ **then**
 - 5: Use Algorithm 2 to obtain α_k satisfying (4) with $\rho = \rho_S$ where $0 < \rho_S < 1/2$.
 - 6: **else**
 - 7: Use Algorithm 3 to obtain α_k satisfying (4) with $\rho = \rho_N$ where $0 < \rho_N < 1$.
 - 8: **end if**
 - 9: $\mathbf{x}_{k+1} = \mathbf{x}_k + \alpha_k \mathbf{d}_k$
 - 10: $k = k + 1$
 - 11: **end while**
 - 12: **return** \mathbf{x}_k
-

3 Theoretical Analyses

We now set out to give complexity guarantees of our Newton-MR variants in several settings. To carry out our analyses, we make several blanket assumptions that will be used throughout this paper. Specific assumptions required for certain results will be stated as needs arise. Our first blanket assumptions are regarding smoothness of the function f , which are widely used throughout the literature.

Assumption 1 (Hessian Boundedness). *The function f is twice continuously differentiable and there exists a constant $0 \leq L_{\mathbf{g}} < \infty$ such that for any $\mathbf{x} \in \mathbb{R}^d$, we have $\|\mathbf{H}(\mathbf{x})\| \leq L_{\mathbf{g}}$.*

Recall that Assumption 1 is equivalent to the usual Lipschitz continuity assumption of the gradient for twice continuously differentiable functions.

Assumption 2 (Lipschitz Continuous Hessian). *There exists a constant $0 \leq L_{\mathbf{H}} < \infty$ such that for any $(\mathbf{x}, \mathbf{y}) \in \mathbb{R}^{d \times d}$, we have*

$$\|\mathbf{H}(\mathbf{x}) - \mathbf{H}(\mathbf{y})\| \leq L_{\mathbf{H}} \|\mathbf{x} - \mathbf{y}\|.$$

Within the Lanczos process, the basis matrix $\mathbf{V}_t \in \mathbb{R}^{d \times t}$ for the Krylov subspace $\mathcal{K}_t(\bar{\mathbf{H}}, \mathbf{g})$ and the symmetric tridiagonal matrix $\mathbf{T}_t \in \mathbb{R}^{t \times t}$, are iteratively generated such that $\mathbf{T}_t = \mathbf{V}_t^{\top} \bar{\mathbf{H}} \mathbf{V}_t$. It is guaranteed by [42, Theorem 3.3] that, prior to the detection of Condition 2, i.e., as long as an NPC direction has not been detected, the matrix \mathbf{T}_t remains positive definite, i.e., $\mathbf{T}_t \succ 0$. In other words, prior to the detection of an NPC detection, MINRES guarantees that $\langle \mathbf{v}, \bar{\mathbf{H}} \mathbf{v} \rangle > 0$ for any $\mathbf{v} \in \mathcal{K}_t(\bar{\mathbf{H}}, \mathbf{g})$. Note that this is simply a property of the MINRES algorithm and holds regardless of the underlying matrix $\bar{\mathbf{H}}$ and the vector \mathbf{g} . Similar to [43, Assumption 3], here we also assume assuming that, as long as Condition 2 has not been detected, \mathbf{T}_t remains uniformly positive definite.

Assumption 3 (Krylov Subspace Regularity). *There is a constant $\sigma > 0$ small enough, such that for any $\mathbf{x} \in \mathbb{R}^d$, before Condition 2 is detected, we have $\mathbf{T}_t \succeq \sigma \mathbf{I}$.*

Assumption 3 is well-motivated by the properties of MINRES and the tridiagonal matrix \mathbf{T}_t and is not restrictive. In fact, as mentioned in [43], if we assume the sub-level sets of the function f are bounded, which is often done in similar literature, e.g., [53, 54, 66], Assumption 3 is trivially satisfied. In the following two examples, we show that the constant σ in Assumption 3 also does not depend on the inexactness ε .

Example 1: Consider Algorithm 1 with

$$\bar{\mathbf{H}} = \begin{bmatrix} L_{\mathbf{g}} + \varepsilon & \\ & -\mu + \varepsilon \end{bmatrix} \quad \text{and} \quad \mathbf{g} = - \begin{bmatrix} 1 \\ 1 \end{bmatrix},$$

where $L_{\mathbf{g}} > \mu$. At $t = 1$, we have

$$\mathbf{v}_1 = \frac{1}{\sqrt{2}} \begin{bmatrix} 1 \\ 1 \end{bmatrix}, \quad \alpha_1 = \frac{L_{\mathbf{g}} - \mu}{2}, \quad \beta_2 = \frac{L_{\mathbf{g}} + \mu}{2} \quad \text{and} \quad \langle \mathbf{r}_0, \bar{\mathbf{H}} \mathbf{r}_0 \rangle = \frac{L_{\mathbf{g}} - \mu}{2},$$

and, at $t = 2$,

$$\mathbf{v}_2 = \frac{1}{\sqrt{2}} \begin{bmatrix} 1 \\ -1 \end{bmatrix}, \quad \alpha_2 = \frac{L_{\mathbf{g}} - \mu + 2\varepsilon}{2} \quad \text{and} \quad \langle \mathbf{r}_1, \bar{\mathbf{H}} \mathbf{r}_1 \rangle = \frac{(L_{\mathbf{g}} - \mu + 2\varepsilon)(L_{\mathbf{g}} + \varepsilon)(-\mu + \varepsilon)}{(L_{\mathbf{g}} + \varepsilon)^2 + (-\mu + \varepsilon)^2}.$$

We consider ε with two different values, namely $\varepsilon < \mu$ and $\varepsilon = \mu$, which amount to indefinite, positive semi-definite, respectively. We show that, in each case, the constant σ does not depend on ε .

($\varepsilon < \mu$): We detect NPC Condition 2 at $t = 2$, i.e. $\langle \mathbf{r}_1, \bar{\mathbf{H}} \mathbf{r}_1 \rangle < 0$. In this case,

$$\mathbf{T}_1 \succeq \alpha_1 \mathbf{I} \triangleq \sigma \mathbf{I},$$

which is independent of ε .

($\mu = \varepsilon$): We detect the zero curvature, at $t = 2$, i.e. $\langle \mathbf{r}_1, \bar{\mathbf{H}}\mathbf{r}_1 \rangle = 0$. We again have

$$\mathbf{T}_1 \succeq \alpha_1 \mathbf{I} \triangleq \sigma \mathbf{I},$$

which is independent of ε .

For $\varepsilon > \mu$, $\bar{\mathbf{H}}$ is positive definite. In this case, as ε grows, the constant σ will also grow with ε . However, we are only interested in the situation when ε is small. So, this case is irrelevant with our analysis.

Example 2: We now empirically verify that the constant σ in Assumption 3 does not depend on the inexactness ε . For this, we construct $\bar{\mathbf{H}}$ as follows. We randomly draw 28 samples from a uniform distribution $U(0, 10)$ and 2 samples from another uniform distribution $U(-1, 0)$ to form a 30 by 30 diagonal matrix \mathbf{D} . Furthermore, we form another diagonal matrix $\mathbf{D}_{\{1,-1\}}$ whose diagonal elements are randomly set to ± 1 . We then construct our matrix $\bar{\mathbf{H}}$ as follows,

$$\bar{\mathbf{H}} = \mathbf{V}\mathbf{D}\mathbf{V}^\top + \varepsilon\mathbf{W}\mathbf{D}_{\{1,-1\}}\mathbf{W}^\top$$

where \mathbf{V} and \mathbf{W} are arbitrary orthonormal matrices, and ε takes the value of $\{1, 0.1, 0.01, 0.001, 0.0001\}$. As we can see from figure 1, with sufficiently small ε , the minimum eigenvalue of \mathbf{T}_t prior to the detection of NPC direction is independent of ε .

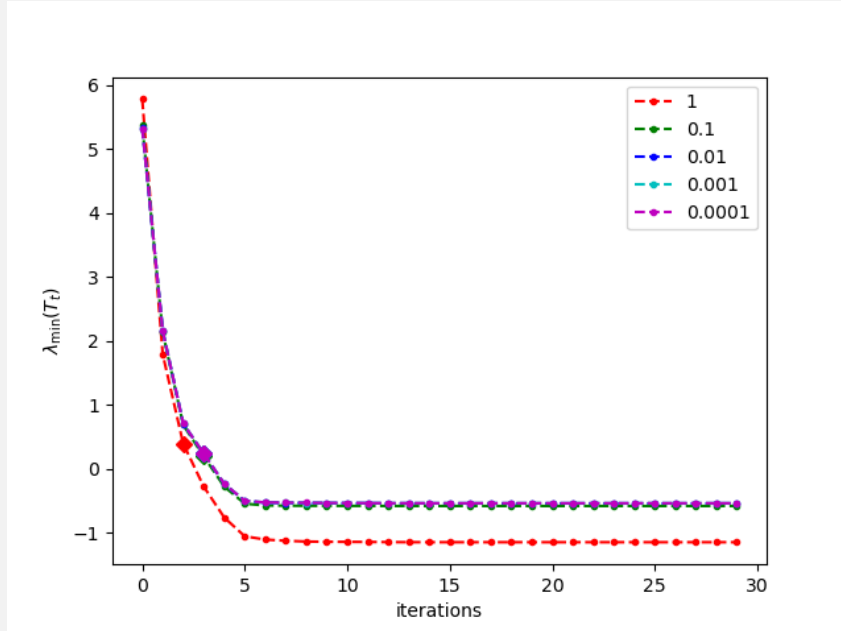


Figure 1: Each dots on the graph is the minimum eigenvalue of \mathbf{T}_t at each iteration. The diamond marker is $\lambda_{\min}(\mathbf{T}_t)$ at the iteration prior to the detection of Condition 2. As it can be seen, decreasing ε has no detectable effect on the value of $\lambda_{\min}(\mathbf{T}_t)$ at such iteration.

3.1 Functions satisfying Polyak-Łojasiewicz Condition

Before exploring broader nonconvex functions, and to set the stage, let us consider a very special class of nonconvex functions, namely those satisfying the Polyak-Łojasiewicz (PL). More specifically, we assume that there is a constant $\mu > 0$ such that

$$\frac{1}{2}\|\mathbf{g}(\mathbf{x})\|^2 \geq \mu(f(\mathbf{x}) - f^*), \quad \forall \mathbf{x} \in \mathbb{R}^d.$$

We show that under Assumptions 1 and 3, Algorithm 4 achieves a linear convergence rate for PL functions. Among Newton-type methods with inexact Hessian information, our work here is, to the best of our knowledge, the first to establish such linear rate for PL functions with mild assumptions.

Prior works on establishing linear convergence of Newton-type methods with inexact Hessian have predominantly focused on (strongly) convex functions. These studies have either assumed that the approximate Hessian remains positive definite [14, 15, 16, 27, 52] or that the gradient lies in the range of Hessian at all times [30]. These stringent assumptions either necessitate highly accurate Hessian approximations or significantly restrict the scope of problems that can be effectively solved. However, these limitations often conflict with what is observed in practice. For instance, the sub-sampled Newton method can effectively solve (strongly) convex finite-sum problems with very crude Hessian approximations using much fewer samples than what the concentration inequalities predict [64]. Similarly, for high-dimensional convex problems where the Hessian matrix is singular and the gradient may not entirely lie in the range of Hessian, Newton’s method remains practically a viable algorithm [51].

The limitations imposed by these stringent assumptions arise from the common practice in previous studies, where the sub-problem solver is treated as a black box, neglecting the opportunity to leverage its inherent properties. In contrast, by tapping into the properties of MINRES, we show that simply requiring Assumptions 1 and 3 allows us to establish the linear convergence of Algorithm 4 under *any amount of inexactness* in the Hessian matrix, effectively bridging the gap between theory and practice in these setting.

Lemma 1. *Consider (3) for any $\varepsilon > 0$ and let Assumptions 1 and 3 hold. Condition 1 implies*

$$\|\mathbf{g}_k\| < \kappa(\eta + L_{\mathbf{g}} + \varepsilon)\|\mathbf{s}_k^{(t-1)}\|,$$

where $\kappa \triangleq (L_{\mathbf{g}} + \varepsilon)/\sigma$.

Proof. Condition 1 gives

$$\eta\|\bar{\mathbf{H}}_k\mathbf{s}_k^{(t-1)}\| > \|\bar{\mathbf{H}}_k\mathbf{r}_k^{(t-1)}\| = \|\bar{\mathbf{H}}_k(\bar{\mathbf{H}}_k\mathbf{s}_k^{(t-1)} + \mathbf{g}_k)\| > \|\bar{\mathbf{H}}_k\mathbf{g}_k\| - \|\bar{\mathbf{H}}_k^2\mathbf{s}_k^{(t-1)}\|.$$

Hence, we have $(\eta + \|\bar{\mathbf{H}}_k\|)\|\bar{\mathbf{H}}_k\mathbf{s}_k^{(t-1)}\| > \|\bar{\mathbf{H}}_k\mathbf{g}_k\|$, which implies

$$(\eta + L_{\mathbf{g}} + \varepsilon)(L_{\mathbf{g}} + \varepsilon)\|\mathbf{s}_k^{(t-1)}\| > \sigma\|\mathbf{g}_k\|,$$

and we get the desired result. \square

Lemmas 2 and 3 show the minimum amount of descent Algorithm 4 can achieve going from $f(\mathbf{x}_k)$ to $f(\mathbf{x}_{k+1})$, when “Type = SOL” and “Type = NPC”, respectively.

Lemma 2. *Under the same assumptions as in Lemma 1, in Algorithm 4 with Type = SOL, we have*

$$f(\mathbf{x}_{k+1}) - f(\mathbf{x}_k) \leq -\frac{2\beta(1-\beta)}{L_{\mathbf{g}}\kappa^2(\eta/\sigma + \kappa)^2}\|\mathbf{g}_k\|^2.$$

Proof. By Assumption 1, we have

$$f(\mathbf{x} + \alpha_k\mathbf{d}_k) - f(\mathbf{x}) \leq \alpha_k\langle\mathbf{d}_k, \mathbf{g}_k\rangle + \frac{\alpha_k^2 L_{\mathbf{g}}}{2}\|\mathbf{d}_k\|^2.$$

Now, the line-search is satisfied if for some $0 < \alpha \leq 1$ we have

$$\alpha_k\langle\mathbf{d}_k, \mathbf{g}_k\rangle + \frac{\alpha_k^2 L_{\mathbf{g}}}{2}\|\mathbf{d}_k\|^2 \leq \alpha_k\beta\langle\mathbf{d}_k, \mathbf{g}_k\rangle,$$

which implies

$$\alpha_k \leq \frac{2(\beta - 1)}{L_{\mathbf{g}}\|\mathbf{d}_k\|^2}\langle\mathbf{d}_k, \mathbf{g}_k\rangle.$$

Since Condition 1 is satisfied, i.e., $\mathbf{d}_k = \mathbf{s}_k^{(t-1)}$, from [42, Theorem 3.8] and Assumption 3, we have

$$\langle\mathbf{d}_k, \mathbf{g}_k\rangle < -\langle\mathbf{d}_k, \bar{\mathbf{H}}_k\mathbf{d}_k\rangle \leq -\sigma\|\mathbf{d}_k\|^2.$$

Hence, the step size returned from the line-search must satisfy

$$\alpha_k \geq \frac{2\sigma(1-\beta)}{L_{\mathbf{g}}}.$$

Substituting back to the inequality from the line-search, we get

$$f(\mathbf{x}_{k+1}) - f(\mathbf{x}_k) \leq \alpha_k \beta \langle \mathbf{d}_k, \mathbf{g}_k \rangle \leq \frac{2\sigma\beta(1-\beta)}{L_{\mathbf{g}}} \langle \mathbf{d}_k, \mathbf{g}_k \rangle \leq -\frac{2\sigma^2\beta(1-\beta)}{L_{\mathbf{g}}} \|\mathbf{d}_k\|^2,$$

which using Lemma 1 gives the desired result. \square

Lemma 3. *Under the same assumptions as in Lemma 1, in Algorithm 4 with Type = NPC, we have*

$$f(\mathbf{x}_{k+1}) - f(\mathbf{x}_k) \leq -\frac{2\beta(1-\beta)(\eta/\sigma)^2}{L_{\mathbf{g}}(\kappa^2 + (\eta/\sigma)^2)} \|\mathbf{g}_k\|^2.$$

Proof. Similar to the proof Lemma 1, for α_k to satisfy (4), we need

$$\alpha_k \langle \mathbf{d}_k, \mathbf{g}_k \rangle + \frac{\alpha_k^2 L_{\mathbf{g}}}{2} \|\mathbf{d}_k\|^2 \leq \alpha_k \beta \langle \mathbf{d}_k, \mathbf{g}_k \rangle,$$

which gives

$$\alpha_k \leq \frac{2(\beta-1)}{L_{\mathbf{g}} \|\mathbf{d}_k\|^2} \langle \mathbf{d}_k, \mathbf{g}_k \rangle.$$

Since Condition 2 is satisfied, i.e., $\mathbf{d}_k = \mathbf{r}_k^{(t-1)}$, from [42, Lemma 3.1], we have $\langle \mathbf{r}_k^{(t-1)}, \mathbf{g}_k \rangle = -\|\mathbf{r}_k^{(t-1)}\|^2$. Hence, the step size returned from the line-search must satisfy

$$\alpha_k \geq \frac{2(1-\beta)}{L_{\mathbf{g}}}.$$

Substituting back to the inequality from the line-search, we get

$$f_{k+1} - f_k \leq \alpha_k \beta \langle \mathbf{d}_k, \mathbf{g}_k \rangle = -\frac{2\beta(1-\beta)}{L_{\mathbf{g}}} \|\mathbf{d}_k^{(t-1)}\|^2.$$

Since Condition 2 has been triggered prior to Condition 1, from [42, Lemma 3.1] and Assumption 1 we have

$$\frac{(L_{\mathbf{g}} + \varepsilon)^2}{\eta^2} \|\mathbf{r}_k^{(t-1)}\|^2 \geq \frac{\|\bar{\mathbf{H}}_k \mathbf{r}_k^{(t-1)}\|^2}{\eta^2} \geq \|\bar{\mathbf{H}}_k \mathbf{p}_k^{(t-1)}\|^2 = \|\mathbf{r}_k^{(t-1)} + \mathbf{g}_k\|^2 = \|\mathbf{g}_k\|^2 - \|\mathbf{r}_k^{(t-1)}\|^2,$$

which implies

$$\|\mathbf{r}_k^{(t-1)}\|^2 \geq \frac{\eta^2}{(L_{\mathbf{g}} + \varepsilon)^2 + \eta^2} \|\mathbf{g}_k\|^2,$$

we get the desired result. \square

Now, putting together Lemmas 1 to 3, we get the linear rate of Algorithm 4 for functions satisfying PL condition.

Theorem 1. *Consider (3) for any $\varepsilon > 0$, Condition 1 for any $\eta > 0$, and let Assumptions 1 and 3 hold. In Algorithm 4, we have*

$$f(\mathbf{x}_{k+1}) - f^* \leq \left(1 - \frac{4\mu\beta(1-\beta)}{L_{\mathbf{g}}}\right) \min \left\{ \frac{1}{\kappa^2(\eta/\sigma + \kappa)^2}, \frac{(\eta/\sigma)^2}{\kappa^2 + (\eta/\sigma)^2} \right\} (f(\mathbf{x}_k) - f^*),$$

where $\kappa \triangleq (L_{\mathbf{g}} + \varepsilon)/\sigma$.

Proof. For each iteration of Algorithm 4, we either have Type = SOL or Type = NPC. Thus, we get

$$f(\mathbf{x}_{k+1}) - f(\mathbf{x}_k) \leq -\frac{2\beta(1-\beta)}{L_{\mathbf{g}}}\min \left\{ \frac{1}{\kappa^2(\eta/\sigma + \kappa)^2}, \frac{(\eta/\sigma)^2}{\kappa^2 + (\eta/\sigma)^2} \right\} \|\mathbf{g}_k\|^2,$$

which using the PL condition gives what is desired. \square

The advantage of Theorem 1 is that it establishes linear convergence of Algorithm 4 for *any* value of ε and η . In other words, regardless of how crude our Hessian approximation or inner problem solution might be, Algorithm 4 still exhibits linear convergence rate for PL functions. This, to a great degree, corroborates what is typically observed in practice when solving, say, strongly convex problems, which can be seen as a sub-class of PL functions. Newton's method remains a convergent algorithm with well-defined iterations, irrespective of the level of approximation used for Hessian or the underlying sub-problem solution [10, 51, 52].

We note that due to our choice of sub-problem inexactness condition, which is suitable for non-convex settings, the above bound does not match those typically obtained for Newton's method in strongly convex problems, where the sub-problem inexactness is commonly measured using relative residual as $\|\mathbf{r}_k^{(t-1)}\| \leq \eta \|\mathbf{g}_k\|$.

3.2 General nonconvex Functions

We now move onto analyzing the convergence of our Newton-MR variants applied to more general nonconvex problems. For this, we first give convergence guarantees of Algorithm 4 both in terms of iteration as well as operation complexities to achieve first-order sub-optimality (2a). We then consider a variant, which comes equipped with favorable complexities to guarantee second-order sub-optimality (2a) and (2b).

3.2.1 First-order Complexity

In this section, we present optimal iteration and operation complexities of Algorithm 4 to achieve first-order approximate optimality guarantee as in (2a).

First-order Iteration Complexity

To provide the first-order iteration complexity of Algorithm 4, we first show that the magnitude of the direction can serve as an estimate on the gradient norm in the next iteration. This is then used to obtain a bound on the worst-case decrease in the objective value. The proof follows closely the line of reasoning in [43, Lemma 7].

Lemma 4. *Suppose Assumptions 1 to 3 are satisfied, Condition 1 holds with $\eta = \theta\sqrt{\varepsilon_{\mathbf{g}}}$ for some $\theta > 0$, and $\varepsilon \leq \sqrt{\varepsilon_{\mathbf{g}}}/(\eta + \sigma)$ in (3). We have*

$$\|\mathbf{d}_k\| \geq c_0 \sqrt{\varepsilon_{\mathbf{g}}} \min\{\|\mathbf{g}(\mathbf{x}_k + \mathbf{d}_k)\|/\varepsilon_{\mathbf{g}}, 1\},$$

where

$$c_0 \triangleq \left(\frac{2\sigma}{(1 + \theta L_{\mathbf{g}}) + \sqrt{(1 + \theta L_{\mathbf{g}})^2 + 2\sigma^2 L_{\mathbf{H}}}} \right).$$

Proof. From Algorithm 4, since Condition 1 is triggered, we have $\text{Type} = \text{SOL}$ and $\mathbf{d}_k = \mathbf{s}_k^{(t-1)}$. From Assumption 3, since $\mathbf{r}_k^{(t-1)} \in \mathcal{K}_t(\bar{\mathbf{H}}_k, \mathbf{g}_k)$, we have

$$\|\mathbf{r}_k^{(t-1)}\| \|\bar{\mathbf{H}}_k \mathbf{r}_k^{(t-1)}\| \geq \langle \mathbf{r}_k^{(t-1)}, \bar{\mathbf{H}}_k \mathbf{r}_k^{(t-1)} \rangle \geq \sigma \|\mathbf{r}_k^{(t-1)}\|^2.$$

With that,

$$\begin{aligned} \|\mathbf{g}(\mathbf{x}_k + \mathbf{d}_k)\| &= \|\mathbf{g}(\mathbf{x}_k + \mathbf{d}_k) - \mathbf{g}_k - \bar{\mathbf{H}}_k \mathbf{d}_k - \mathbf{r}_k^{(t-1)}\| \\ &\leq \|\mathbf{g}(\mathbf{x}_k + \mathbf{d}_k) - \mathbf{g}_k - \mathbf{H}_k \mathbf{d}_k - \mathbf{E}_k \mathbf{d}_k\| + \|\mathbf{r}_k^{(t-1)}\| \\ &\leq \frac{L_{\mathbf{H}}}{2} \|\mathbf{d}_k\|^2 + \varepsilon \|\mathbf{d}_k\| + \frac{\|\bar{\mathbf{H}}_k \mathbf{r}_k^{(t-1)}\|}{\sigma} \\ &\leq \frac{L_{\mathbf{H}}}{2} \|\mathbf{d}_k\|^2 + \varepsilon \|\mathbf{d}_k\| + \frac{\eta \|\bar{\mathbf{H}}_k \mathbf{d}_k\|}{\sigma} \\ &\leq \frac{L_{\mathbf{H}}}{2} \|\mathbf{d}_k\|^2 + \varepsilon \|\mathbf{d}_k\| + \frac{\eta \|\mathbf{H}_k \mathbf{d}_k\| + \eta \|\mathbf{E}_k \mathbf{d}_k\|}{\sigma} \\ &\leq \frac{L_{\mathbf{H}}}{2} \|\mathbf{d}_k\|^2 + \varepsilon \|\mathbf{d}_k\| + \frac{\eta L_{\mathbf{g}} \|\mathbf{d}_k\|}{\sigma} + \frac{\eta \varepsilon \|\mathbf{d}_k\|}{\sigma} \\ &= \frac{L_{\mathbf{H}}}{2} \|\mathbf{d}_k\|^2 + \frac{\eta L_{\mathbf{g}} \|\mathbf{d}_k\|}{\sigma} + \left(\frac{\eta + \sigma}{\sigma} \right) \varepsilon \|\mathbf{d}_k\|. \end{aligned}$$

With $\varepsilon \leq \sqrt{\varepsilon_{\mathbf{g}}}/(\eta + \sigma)$ and $\eta = \theta\sqrt{\varepsilon_{\mathbf{g}}}$ for $\theta > 0$, we have

$$0 \leq \sigma L_{\mathbf{H}} \|\mathbf{d}_k\|^2 + 2(1 + \theta L_{\mathbf{g}}) \sqrt{\varepsilon_{\mathbf{g}}} \|\mathbf{d}_k\| - 2\sigma \|\mathbf{g}(\mathbf{x}_k + \mathbf{d}_k)\|,$$

By solving the previous quadratic inequality, we obtain

$$\begin{aligned} \|\mathbf{d}_k\| &\geq \frac{-2(1 + \theta L_{\mathbf{g}}) \sqrt{\varepsilon_{\mathbf{g}}} + \sqrt{4(1 + \theta L_{\mathbf{g}})^2 \varepsilon_{\mathbf{g}} + 8\sigma^2 L_{\mathbf{H}} \|\mathbf{g}(\mathbf{x}_k + \mathbf{d}_k)\|}}{2\sigma L_{\mathbf{H}}} \\ &= \left(\frac{-(1 + \theta L_{\mathbf{g}}) + \sqrt{(1 + \theta L_{\mathbf{g}})^2 + 2\sigma^2 L_{\mathbf{H}} \|\mathbf{g}(\mathbf{x}_k + \mathbf{d}_k)\|/\varepsilon_{\mathbf{g}}}}{\sigma L_{\mathbf{H}}} \right) \sqrt{\varepsilon_{\mathbf{g}}} \\ &= \left(\frac{2\sigma \|\mathbf{g}(\mathbf{x}_k + \mathbf{d}_k)\|/\varepsilon_{\mathbf{g}}}{(1 + \theta L_{\mathbf{g}}) + \sqrt{(1 + \theta L_{\mathbf{g}})^2 + 2\sigma^2 L_{\mathbf{H}} \|\mathbf{g}(\mathbf{x}_k + \mathbf{d}_k)\|/\varepsilon_{\mathbf{g}}}} \right) \sqrt{\varepsilon_{\mathbf{g}}} \\ &\geq \left(\frac{2\sigma}{(1 + \theta L_{\mathbf{g}}) + \sqrt{(1 + \theta L_{\mathbf{g}})^2 + 2\sigma^2 L_{\mathbf{H}}}} \right) \sqrt{\varepsilon_{\mathbf{g}}} \min\{\|\mathbf{g}(\mathbf{x}_k + \mathbf{d}_k)\|/\varepsilon_{\mathbf{g}}, 1\}. \end{aligned}$$

□

With the lemma above, we can now give the least amount of decrease in f for when `Type = SOL`.

Lemma 5. *Suppose Assumptions 1 to 3 are satisfied, Condition 1 holds with $\eta = \theta\sqrt{\varepsilon_{\mathbf{g}}}$ for some $\theta > 0$, and*

$$\varepsilon \leq \min\{(1 - 2\rho_S)\sigma/2, \sqrt{\varepsilon_{\mathbf{g}}}/(\eta + \sigma)\},$$

in (3). We have

$$f(\mathbf{x}_{k+1}) \leq f(\mathbf{x}_k) - \min\{c_1, c_2 \|\mathbf{g}_{k+1}\|^2/\varepsilon_{\mathbf{g}}, c_2 \varepsilon_{\mathbf{g}}\},$$

where, for $0 < \rho_S < 1/2$,

$$c_1 \triangleq \rho_S \sigma \left(\frac{3(1 - 2\rho_S)\sigma}{2L_{\mathbf{H}}} \right)^2, \quad c_2 \triangleq \rho_S \sigma c_0^2,$$

and c_0 from lemma 4.

Proof. From Algorithm 4, since Condition 1 is triggered, we have `Type = SOL` and $\mathbf{d}_k = \mathbf{s}_k^{(t-1)}$. Using the smoothness assumption, we have

$$\begin{aligned} f(\mathbf{x}_{k+1}) - f(\mathbf{x}_k) &\leq \alpha_k \langle \mathbf{d}_k, \mathbf{g}_k \rangle + \frac{\alpha_k^2}{2} \langle \mathbf{d}_k, \mathbf{H}_k \mathbf{d}_k \rangle + \frac{\alpha_k^3 L_{\mathbf{H}}}{6} \|\mathbf{d}_k\|^3 \\ &= \alpha_k \langle \mathbf{d}_k, \mathbf{g}_k \rangle + \frac{\alpha_k^2}{2} \langle \mathbf{d}_k, \bar{\mathbf{H}}_k \mathbf{d}_k \rangle - \frac{\alpha_k^2}{2} \langle \mathbf{d}_k, \mathbf{E}_k \mathbf{d}_k \rangle + \frac{\alpha_k^3 L_{\mathbf{H}}}{6} \|\mathbf{d}_k\|^3 \\ &= \left(\alpha_k - \frac{\alpha_k^2}{2} \right) \langle \mathbf{d}_k, \mathbf{g}_k \rangle + \frac{\alpha_k^2}{2} (\langle \mathbf{d}_k, \mathbf{g}_k \rangle + \langle \mathbf{d}_k, \bar{\mathbf{H}}_k \mathbf{d}_k \rangle) - \frac{\alpha_k^2}{2} \langle \mathbf{d}_k, \mathbf{E}_k \mathbf{d}_k \rangle + \frac{\alpha_k^3 L_{\mathbf{H}}}{6} \|\mathbf{d}_k\|^3. \end{aligned}$$

Since $-\langle \mathbf{d}_k, \mathbf{E}_k \mathbf{d}_k \rangle < \varepsilon \|\mathbf{d}_k\|^2$ and $\langle \mathbf{d}_k, \mathbf{g}_k \rangle < -\langle \mathbf{d}_k, \bar{\mathbf{H}}_k \mathbf{d}_k \rangle$ [42, Theorem 3.8], it follows that

$$\begin{aligned} f(\mathbf{x}_{k+1}) - f(\mathbf{x}_k) &\leq \left(\alpha_k - \frac{\alpha_k^2}{2} \right) \langle \mathbf{d}_k, \mathbf{g}_k \rangle + \frac{\alpha_k^2 \varepsilon}{2} \|\mathbf{d}_k\|^2 + \frac{\alpha_k^3 L_{\mathbf{H}}}{6} \|\mathbf{d}_k\|^3 \\ &\leq \left(\alpha_k - \frac{\alpha_k}{2} \right) \langle \mathbf{d}_k, \mathbf{g}_k \rangle + \frac{\alpha_k \varepsilon}{2} \|\mathbf{d}_k\|^2 + \frac{\alpha_k^3 L_{\mathbf{H}}}{6} \|\mathbf{d}_k\|^3, \end{aligned}$$

where the last inequality holds since $\alpha_k \leq 1$. Now, the line-search is satisfied if for some $0 < \alpha_k \leq 1$ we have

$$\left(\alpha_k - \frac{\alpha_k}{2} \right) \langle \mathbf{d}_k, \mathbf{g}_k \rangle + \frac{\alpha_k \varepsilon}{2} \|\mathbf{d}_k\|^2 + \frac{\alpha_k^3 L_{\mathbf{H}}}{6} \|\mathbf{d}_k\|^3 \leq \alpha_k \rho_S \langle \mathbf{d}_k, \mathbf{g}_k \rangle,$$

which gives

$$\alpha_k \leq \sqrt{\frac{-3(1 - 2\rho_S) \langle \mathbf{d}_k, \mathbf{g}_k \rangle - 3\varepsilon \|\mathbf{d}_k\|^2}{L_{\mathbf{H}} \|\mathbf{d}_k\|^3}}.$$

With Assumption 3, $\langle \mathbf{d}_k, \mathbf{g}_k \rangle \leq -\sigma \|\mathbf{d}_k\|^2$ and

$$\sqrt{\frac{3((1-2\rho_S)\sigma - \varepsilon)}{L_{\mathbf{H}}\|\mathbf{d}_k\|}} = \sqrt{\frac{3(1-2\rho_S)\sigma\|\mathbf{d}_k\|^2 - 3\varepsilon\|\mathbf{d}_k\|^2}{L_{\mathbf{H}}\|\mathbf{d}_k\|^3}} \leq \sqrt{\frac{-3(1-2\rho_S)\langle \mathbf{d}_k, \mathbf{g}_k \rangle - 3\varepsilon\|\mathbf{d}_k\|^2}{L_{\mathbf{H}}\|\mathbf{d}_k\|^3}}.$$

Hence, the step size returned from the line-search must satisfy

$$\alpha_k \geq \min \left\{ 1, \sqrt{\frac{3((1-2\rho_S)\sigma - \varepsilon)}{L_{\mathbf{H}}\|\mathbf{d}_k\|}} \right\},$$

which from $\varepsilon \leq (1-2\rho_S)\sigma/2$, gives

$$\alpha_k \geq \min \left\{ 1, \sqrt{\frac{3(1-2\rho_S)\sigma}{2L_{\mathbf{H}}\|\mathbf{d}_k\|}} \right\}.$$

Now, we consider two cases. If

$$\|\mathbf{d}_k\| \geq \frac{3(1-2\rho_S)\sigma}{2L_{\mathbf{H}}},$$

then

$$\alpha_k \geq \sqrt{\frac{3(1-2\rho_S)\sigma}{2L_{\mathbf{H}}\|\mathbf{d}_k\|}},$$

which from the line-search, it follows that

$$\begin{aligned} f(\mathbf{x}_{k+1}) - f(\mathbf{x}_k) &\leq \rho_S \alpha_k \langle \mathbf{g}_k, \mathbf{d}_k \rangle \leq -\rho_S \alpha_k \sigma \|\mathbf{d}_k\|^2 \\ &\leq -\rho_S \sigma \sqrt{\frac{3(1-2\rho_S)\sigma}{2L_{\mathbf{H}}}} \|\mathbf{d}_k\|^{3/2} \leq -\rho_S \sigma \left(\frac{3(1-2\rho_S)\sigma}{2L_{\mathbf{H}}} \right)^2. \end{aligned}$$

Otherwise, $\alpha_k = 1$, and by Lemma 4 we get

$$f(\mathbf{x}_{k+1}) - f(\mathbf{x}_k) \leq -\rho_S \sigma \|\mathbf{d}_k\|^2 \leq -\rho_S \sigma c_0^2 \min\{\|\mathbf{g}_{k+1}\|^2/\varepsilon_{\mathbf{g}}, \varepsilon_{\mathbf{g}}\}.$$

Putting together these two cases, we get the desired result. \square

Next, we investigate the behavior of Algorithm 4 when Condition 2 is detected, i.e., $\text{Type} = \text{NPC}$ and $\mathbf{d}_k = \mathbf{r}_k^{(t-1)}$. In this case, since Condition 2 is triggered prior to Condition 1, we must have

$$\|\mathbf{r}_k^{(t-1)}\| \geq \frac{\eta}{\sqrt{(L_{\mathbf{g}} + \varepsilon)^2 + \eta^2}} \|\mathbf{g}_k\|.$$

With $\eta = \theta\sqrt{\varepsilon_{\mathbf{g}}}$, this gives the first impression that the residual norm $\|\mathbf{r}_k^{(t-1)}\|$ must somehow depend on $\varepsilon_{\mathbf{g}}$, i.e., $\|\mathbf{r}_k^{(t-1)}\| \in \Omega(\sqrt{\varepsilon_{\mathbf{g}}})$. However, the existence of an $\varepsilon_{\mathbf{g}}$ -independent lower-bound, $\|\mathbf{r}_k^{(t-1)}\| \geq \|(\mathbf{I} - \bar{\mathbf{H}}_k \bar{\mathbf{H}}_k^\dagger) \mathbf{g}_k\|$, which is in fact non-trivial when \mathbf{g}_k is not entirely in the range of $\bar{\mathbf{H}}_k$, suggests that $\|\mathbf{r}_k^{(t-1)}\|$ should not depend on $\varepsilon_{\mathbf{g}}$. This is in fact thoroughly justified in [43] using the construction of the MINRES algorithm as well as through several empirical observations. We also note that the constant ω does not depend on the inexactness ε , as shown in the following two examples.

Example 3: Consider Algorithm 1 with

$$\bar{\mathbf{H}} = \begin{bmatrix} L_{\mathbf{g}} + \varepsilon & \\ & -\mu + \varepsilon \end{bmatrix} \quad \text{and} \quad \mathbf{g} = - \begin{bmatrix} 1 \\ h \end{bmatrix},$$

where $L_{\mathbf{g}} > \mu$. At $t = 1$, we have

$$\mathbf{v}_1 = \frac{1}{\sqrt{1+h^2}} \begin{bmatrix} 1 \\ h \end{bmatrix}, \quad \alpha_1 = \frac{L_{\mathbf{g}} + \varepsilon + (-\mu + \varepsilon)h^2}{1+h^2}, \quad \beta_2 = \frac{(L_{\mathbf{g}} + \mu)h}{1+h^2},$$

$$\langle \mathbf{r}_0, \bar{\mathbf{H}}\mathbf{r}_0 \rangle = \frac{L_{\mathbf{g}} + \varepsilon + (-\mu + \varepsilon)h^2}{1+h^2} \quad \text{and} \quad \frac{\|\mathbf{r}_0\|}{\|\mathbf{g}\|} = 1$$

and, at $t = 2$,

$$\mathbf{v}_2 = \frac{1}{\sqrt{1+h^2}} \begin{bmatrix} h \\ -1 \end{bmatrix}, \quad \alpha_2 = \frac{(L_{\mathbf{g}} + \varepsilon)h^2 - \mu + \varepsilon}{1+h^2}$$

$$\langle \mathbf{r}_1, \bar{\mathbf{H}}\mathbf{r}_1 \rangle = \frac{(L_{\mathbf{g}} + \varepsilon + (-\mu + \varepsilon)h^2)(L_{\mathbf{g}} + \varepsilon)(-\mu + \varepsilon)}{(L_{\mathbf{g}} + \varepsilon)^2 + (-\mu + \varepsilon)^2h^2}$$

and

$$\frac{\|\mathbf{r}_1\|}{\|\mathbf{g}\|} = \frac{(L_{\mathbf{g}} + \mu)h}{\sqrt{(1+h^2)((L_{\mathbf{g}} + \varepsilon)^2 + (-\mu + \varepsilon)^2h^2)}}.$$

Again, we examine each case, namely $\varepsilon < \mu$, $\varepsilon > \mu$ and $\varepsilon = \mu$.

($\mu > \varepsilon$) To detect Condition 2 at the first iteration, we must have $h^2 > -(L_{\mathbf{g}} + \varepsilon)/(-\mu + \varepsilon)$ in which case $\|\mathbf{r}_0\| = \|\mathbf{g}\|$. Otherwise, we have $h^2 \leq -(L_{\mathbf{g}} + \varepsilon)/(-\mu + \varepsilon)$ and Condition 2 is detected at the second iteration. In this case, the relative residual is

$$\begin{aligned} \frac{\|\mathbf{r}_1\|}{\|\mathbf{g}\|} &= \frac{(L_{\mathbf{g}} + \mu)h}{\sqrt{(1+h^2)((L_{\mathbf{g}} + \varepsilon)^2 + (-\mu + \varepsilon)^2h^2)}} \\ &\geq \frac{(L_{\mathbf{g}} + \mu)h}{\sqrt{(1+h^2)(L_{\mathbf{g}} + \varepsilon)(L_{\mathbf{g}} + \mu)}} \geq \frac{h}{\sqrt{1+h^2}}. \end{aligned}$$

($\mu = \varepsilon$) We detect zero curvature at the second iteration, with relative residual being the same as the case before,

$$\frac{\|\mathbf{r}_1\|}{\|\mathbf{g}\|} \geq \frac{h}{\sqrt{1+h^2}}.$$

($\varepsilon > \mu$) The matrix $\bar{\mathbf{H}}$ is positive definite. No NPC Condition 2 will be detected.

In each case above, the relative residuals are independent of ε

Example 4: The setting is exactly the same as Example 2. This time, we are considering the relative residual $\|\mathbf{r}_k^{(t-1)}\|/\|\mathbf{g}_k\|$ when Condition 2 is triggered. As shown in Figure 2, decreasing ε has no detectable effect on the relative residual when Condition 2 is detected.

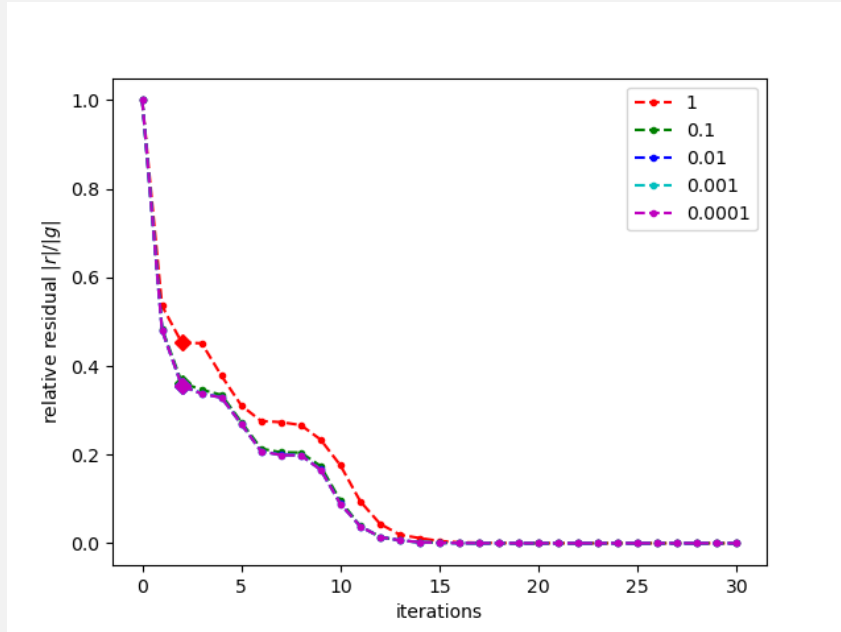


Figure 2: Each dots on the graph is the relative residual at each iteration. The diamond marker is the relative residual $\|\mathbf{r}_k^{(t-1)}\|/\|\mathbf{g}_k\|$ when Condition 2 is triggered. As it can be seen, decreasing ε has no detectable effect on $\|\mathbf{r}_k^{(t-1)}\|/\|\mathbf{g}_k\|$ at such iteration.

This leads us to an assumption similar to [43, Assumption 4].

Assumption 4. *There exists some $\omega > 0$ such that for any \mathbf{x}_k from Algorithm 4, the NPC direction satisfies $\|\mathbf{r}_k^{(t-1)}\| \geq \omega \|\mathbf{g}_k\|$.*

Using Assumption 4, we can get a bound for decrease in f using the NPC direction.

Lemma 6. *Suppose Assumptions 2 and 4 are satisfied, Condition 2 holds, and $\varepsilon \leq 1 - \rho_N$ in (3) for some $0 < \rho_N < 1$. We have*

$$f(\mathbf{x}_{k+1}) \leq f(\mathbf{x}_k) - c_3 \|\mathbf{g}_k\|^{3/2},$$

where

$$c_3 \triangleq \rho_N \omega^{3/2} \sqrt{\frac{3(1 - \rho_N)}{L_{\mathbf{H}}}}.$$

Proof. From Algorithm 4, since Condition 2 is triggered, we have $\text{Type} = \text{NPC}$ and $\mathbf{d}_k = \mathbf{r}_k^{(t-1)}$. By Assumption 2, we have

$$\begin{aligned} f(\mathbf{x}_{k+1}) - f(\mathbf{x}_k) &\leq \alpha_k \langle \mathbf{d}_k, \mathbf{g}_k \rangle + \frac{\alpha_k^2}{2} \langle \mathbf{d}_k, \mathbf{H}_k \mathbf{d}_k \rangle + \frac{\alpha_k^3 L_{\mathbf{H}}}{6} \|\mathbf{d}_k\|^3 \\ &\leq \alpha_k \langle \mathbf{d}_k, \mathbf{g}_k \rangle + \frac{\alpha_k^2}{2} \langle \mathbf{d}_k, \bar{\mathbf{H}}_k \mathbf{d}_k \rangle + \frac{\alpha_k^3 L_{\mathbf{H}}}{6} \|\mathbf{d}_k\|^3 + \frac{\alpha_k^2}{2} \|\mathbf{d}_k\|^2 \varepsilon. \end{aligned}$$

By Condition 2, $\langle \mathbf{d}_k, \bar{\mathbf{H}}_k \mathbf{d}_k \rangle < 0$. From [42, Lemma 3.1], we also have $\langle \mathbf{d}_k, \mathbf{g}_k \rangle = -\|\mathbf{d}_k\|^2$, and hence

$$\begin{aligned} f(\mathbf{x}_{k+1}) - f(\mathbf{x}_k) &\leq -\alpha_k \|\mathbf{d}_k\|^2 + \frac{\alpha_k^3 L_{\mathbf{H}}}{6} \|\mathbf{d}_k\|^3 + \frac{\alpha_k^2}{2} \|\mathbf{d}_k\|^2 \varepsilon \\ &\leq -\alpha_k \|\mathbf{d}_k\|^2 + \frac{\alpha_k^3 L_{\mathbf{H}}}{6} \|\mathbf{d}_k\|^3 + \frac{\alpha_k^2}{2} \|\mathbf{d}_k\|^2 \varepsilon. \end{aligned}$$

Now, the line-search is satisfied if for some $0 < \alpha \leq 1$ we have

$$-\alpha_k \|\mathbf{d}_k\|^2 + \frac{\alpha_k^3 L_{\mathbf{H}}}{6} \|\mathbf{d}_k\|^3 + \frac{\alpha_k^2}{2} \|\mathbf{d}_k\|^2 \varepsilon \leq \alpha_k \rho_N \langle \mathbf{d}_k, \mathbf{g}_k \rangle = -\alpha_k \rho_N \|\mathbf{d}_k\|^2,$$

which gives

$$\alpha_k \geq \sqrt{\frac{6((1 - \varepsilon/2) - \rho_N)}{L_{\mathbf{H}} \|\mathbf{d}_k\|}}.$$

With $\varepsilon \leq 1 - \rho_N$,

$$\alpha_k \geq \sqrt{\frac{3(1 - \rho_N)}{L_{\mathbf{H}} \|\mathbf{d}_k\|}},$$

and hence

$$\begin{aligned} f(\mathbf{x}_{k+1}) - f(\mathbf{x}_k) &\leq \alpha_k \rho_N \langle \mathbf{d}_k, \mathbf{g}_k \rangle \leq -\rho_N \sqrt{\frac{3(1 - \rho_N)}{L_{\mathbf{H}} \|\mathbf{d}_k\|}} \|\mathbf{d}_k\|^2 \\ &\leq -\rho_N \sqrt{\frac{3(1 - \rho_N)}{L_{\mathbf{H}}}} \|\mathbf{d}_k\|^{3/2} \leq -\rho_N \omega^{3/2} \sqrt{\frac{3(1 - \rho_N)}{L_{\mathbf{H}}}} \|\mathbf{g}_k\|^{3/2} \end{aligned}$$

□

Theorem 2 gives the optimal first-order iteration complexity of Algorithm 4 to achieve (2a), which matches that of the exact algorithm given in [43, Theorem 3]. The proof is similar to that of [43, Theorem 3], and is hence omitted.

Theorem 2 (Optimal Iteration Complexity of Algorithm 4). *Under Assumptions 1 to 4, with $\eta = \theta\sqrt{\varepsilon_{\mathbf{g}}}$ for some $\theta > 0$ in Condition 1, and ε in (3) satisfying*

$$\varepsilon \leq \min \left\{ \frac{\sqrt{\varepsilon_{\mathbf{g}}}}{\eta + \sigma}, \frac{\sigma(1 - 2\rho_S)}{2}, 1 - \rho_N \right\},$$

after at most

$$K \triangleq \frac{(f(\mathbf{x}_0) - f^*)\varepsilon_{\mathbf{g}}^{-3/2}}{\min\{c_1, c_2, c_3\}},$$

iterations of Algorithm 4, the approximate first-order optimality (2a) is satisfied. Here c_1 , c_2 and c_3 are defined in Lemmas 4 to 6, and ρ_N and ρ_S are the line-search parameters from Algorithm 4.

First-order Operation Complexity

We now provide an optimal upper bound on the number of gradient and Hessian-vector product evaluations, i.e., operation complexity, required of Algorithm 4 to achieve first-order sub-optimality (2a). A key ingredient in our analysis is understanding the interplay between our noise model (3) and the spectrum of the exact Hessian $\mathbf{H}(\mathbf{x})$. This involves examining the implications of approximating the Hessian in relation to the underlying assumption required for establishing a corresponding result with the exact Hessian in [43].

To enhance clarity, given the complexity of the notation involved in our analysis, we now introduce a new set of symbols that we will use throughout this section.

Notation Used in This Section

The interplay between the Hessian and the gradient plays a central role in establishing the complexity of Newton-MR. This interplay is captured by the notion of \mathbf{g} -relevant eigenvalues/eigenvectors of the (inexact) Hessian matrix. Recall from [43, Section 2.2] that an eigenvalue of \mathbf{H} is called \mathbf{g} -relevant if its associate eigenvectors are not orthogonal to \mathbf{g} . If the dimension of the eigenspace of a \mathbf{g} -relevant eigenvalue is larger than one, without loss of generality we can consider any basis where \mathbf{g} is orthogonal to all but exactly one basis vector. Consequently, we can consider the eigendecomposition of \mathbf{H} as

$$\mathbf{H} = [\mathbf{S} \ \mathbf{S}^\perp] \begin{bmatrix} \mathbf{Z} & \\ & \mathbf{Z}^\perp \end{bmatrix} [\mathbf{S} \ \mathbf{S}^\perp]^\top$$

where \mathbf{Z} is the diagonal matrix containing only the non-zero \mathbf{g} -relevant eigenvalues with associated eigenvectors in \mathbf{S} , and \mathbf{Z}^\perp contains all the remaining eigenvalues (with multiplicities) with the corresponding eigenvectors collected in \mathbf{S}^\perp .

Let $\Upsilon(\mathbf{H}, \mathbf{g})$ be the set of distinct \mathbf{g} -relevant eigenvalues of \mathbf{H} ,

$$\Upsilon(\mathbf{H}, \mathbf{g}) = \{\zeta_1, \zeta_2, \dots, \zeta_{\phi-1}, \zeta_\phi\},$$

with $\zeta_1 > \zeta_2 > \dots > \zeta_{\phi_+} > 0$ and $0 > \zeta_{\phi_+ + \phi_0 + 1} > \dots > \zeta_{\phi-1} > \zeta_\phi$ where $\phi \triangleq |\Upsilon(\mathbf{H}, \mathbf{g})| = \phi_+ + \phi_- + \phi_0$ is the number of distinct \mathbf{g} -relevant eigenvalues of \mathbf{H} , ϕ_+ , ϕ_- and ϕ_0 , respectively, denote the number of distinct positive, negative and zero \mathbf{g} -relevant eigenvalues of \mathbf{H} (clearly $\phi_0 \in \{0, 1\}$). By \mathbf{S}_{i+} , we denote a submatrix of \mathbf{S} whose columns correspond to the i^{th} largest positive \mathbf{g} -relevant eigenvalues of \mathbf{H} . Similarly, the submatrix of \mathbf{S} whose columns are associated with the most negative \mathbf{g} -relevant eigenvalues are denoted by \mathbf{S}_{j-} .

We refer to the eigenvalues/eigenvectors of \mathbf{H} , irrespective of \mathbf{g} -relevance, by using “tilde”. For examples the full spectrum of \mathbf{H} is denoted as as,

$$\rho(\mathbf{H}) = \{\tilde{\zeta}_1, \tilde{\zeta}_2, \dots, \tilde{\zeta}_{d-1}, \tilde{\zeta}_d\},$$

where $\tilde{\zeta}_1 \geq \tilde{\zeta}_2 \geq \dots \geq \tilde{\zeta}_{d-1} \geq \tilde{\zeta}_d$.

We define a function

$$\Phi(\cdot) : \{1, 2, \dots, \phi - 1, \phi\} \rightarrow \{1, 2, \dots, d - 1, d\},$$

that maps from the index set corresponding to $\Upsilon(\mathbf{H}, \mathbf{g})$ to that of $\rho(\mathbf{H})$ such that $\Phi(k)$ is the maximum index of the eigenvalue ζ_k in $\rho(\mathbf{H})$ if ζ_k is non-negative, or the minimum index of the eigenvalue ζ_k in $\rho(\mathbf{H})$, if ζ_k is negative. That is,

$$\Phi(k) \triangleq \begin{cases} \sum_{i=1}^d \mathbb{1}_{\{\tilde{\zeta}_i \geq \zeta_k\}}, & \text{if } \zeta_k \geq 0, \\ 1 + \sum_{i=1}^d \mathbb{1}_{\{\tilde{\zeta}_i > \zeta_k\}}, & \text{if } \zeta_k < 0. \end{cases}$$

Example

Consider $\mathbf{A} = \text{diag}(5, 4, 3, 3, 1, 1, 1, 0, 0, -1, -1, -1, -1)$, and $\mathbf{b} = \mathbf{e}_1 + \mathbf{e}_3 + \mathbf{e}_6 + \mathbf{e}_9 + \mathbf{e}_{11}$. Hence, $\Upsilon(\mathbf{A}, \mathbf{b}) = \{5, 3, 1, 0, -1\}$, which gives $\phi = 5$, $\phi_+ = 3$, $\phi_0 = 1$ and $\phi_- = 1$. Furthermore, $\Phi(1) = 1$, $\Phi(2) = 4$, $\Phi(3) = 7$, $\Phi(4) = 9$, and $\Phi(5) = 10$.

For any $1 \leq k \leq \phi$, we must have $\zeta_k = \tilde{\zeta}_{\Phi(k)}$, by definition. If $\zeta_k \geq 0$, $\tilde{\zeta}_{\Phi(k)+1}$ represents the subsequent distinct, and smaller, eigenvalue of \mathbf{H} (not necessarily \mathbf{g} -relevant); otherwise if $\zeta_k < 0$, $\tilde{\zeta}_{\Phi(k)-1}$ indicates the preceding distinct, and larger, eigenvalue of \mathbf{H} (not necessarily \mathbf{g} -relevant). We will also use the same notational conventions for eigenvectors, i.e., \mathbf{s}_k and $\tilde{\mathbf{s}}_{\Phi(k)}$. Similarly, the eigendecomposition of inexact Hessian $\bar{\mathbf{H}}$ is denoted by

$$\bar{\mathbf{H}} = [\mathbf{U} \quad \mathbf{U}^\perp] \begin{bmatrix} \Lambda & \\ & \Lambda^\perp \end{bmatrix} [\mathbf{U} \quad \mathbf{U}^\perp]^\top,$$

where Λ contains non-zero \mathbf{g} -relevant eigenvalues with their corresponding eigenvectors in \mathbf{U} . The submatrices \mathbf{U}_{i+} and \mathbf{U}_{j-} are defined for $\bar{\mathbf{H}}$ similarly to their counterparts for \mathbf{H} .

The set of \mathbf{g} -relevant eigenvalues of $\bar{\mathbf{H}}$ is denoted by

$$\Upsilon(\bar{\mathbf{H}}, \mathbf{g}) = \{\lambda_1, \lambda_2, \dots, \lambda_{\psi-1}, \Lambda\}.$$

where $\psi \triangleq |\Upsilon(\bar{\mathbf{H}}, \mathbf{g})| = \psi_+ + \psi_- + \psi_0$, and ψ_+ , ψ_- , and ψ_0 have similar meanings as their counterparts above. Again, the eigenvalues/eigenvectors of $\bar{\mathbf{H}}(\mathbf{x})$, irrespective of \mathbf{g} -relevance, are denoted using “tilde”. We define the spectrum of $\bar{\mathbf{H}}$ to be

$$\rho(\bar{\mathbf{H}}) = \{\tilde{\lambda}_1, \tilde{\lambda}_2, \dots, \tilde{\lambda}_{d-1}, \tilde{\lambda}_d\},$$

and the function

$$\Psi(\cdot) : \{1, 2, \dots, \psi - 1, \psi\} \rightarrow \{1, 2, \dots, d - 1, d\},$$

that maps from the index of $\Upsilon(\bar{\mathbf{H}}, \mathbf{g})$ to the index of $\rho(\bar{\mathbf{H}})$ in the same manner as $\Phi(\cdot)$.

The maps Ψ and Φ will conveniently allow us to refer back and forth between \mathbf{g} -relevant eigenvectors and the non- \mathbf{g} -relevant ones. We now prove a couple of important properties of the function $\Phi(\cdot)$, which we will utilise in our lemmas to follow. Note that, what is true of $\Phi(\cdot)$ is also true of $\Psi(\cdot)$, since they differ only in their respective domain.

Lemma 7. *The map $\Phi(\cdot)$ has a unique left inverse, i.e., there exists a function $\Phi^\dagger : \{1, 2, \dots, d - 1, d\} \rightarrow \{1, 2, \dots, \phi - 1, \phi\}$ such that $\Phi^\dagger(\Phi(k)) = k$ for $1 \leq k \leq \phi$.*

Proof. It suffices to show that $\Phi(\cdot)$ is one-to-one, i.e., injective. Let k and k' , in $\{1, \dots, \phi\}$, be two distinct elements. By the definition of $\Upsilon(\mathbf{H}, \mathbf{g})$, we must have $\zeta_k \neq \zeta_{k'}$. Furthermore, by the definition of the function $\Phi(\cdot)$, we have $\zeta_k = \tilde{\zeta}_{\Phi(k)}$ and $\zeta_{k'} = \tilde{\zeta}_{\Phi(k')}$, which implies $\tilde{\zeta}_{\Phi(k)} \neq \tilde{\zeta}_{\Phi(k')}$. Distinct eigenvalues can only have distinct indices. Hence $\Phi(k) \neq \Phi(k')$. \square

Lemma 8. *For $1 \leq j \leq d$, if $\tilde{\zeta}_j$ is \mathbf{g} -relevant, then there exists a unique index k , where $1 \leq k \leq \phi$, such that $\tilde{\zeta}_j = \tilde{\zeta}_{\Phi(k)} = \zeta_k$.*

Proof. Since $\tilde{\zeta}_j \in \rho(\mathbf{H})$ is \mathbf{g} -relevant, there must be $\zeta_k \in \Upsilon(\mathbf{H}, \mathbf{g})$, such that $\tilde{\zeta}_j = \zeta_k$. By Lemma 7 and the definitions of $\Upsilon(\mathbf{H}, \mathbf{g})$ and the function Φ , we also have $\tilde{\zeta}_{\Phi(k)} = \zeta_k$ and k is unique. \square

In order to establish operation complexity, [43] makes use of a rather mild, yet key, assumption, which essentially requires that, for any given iterate, unless $\mathbf{g} \notin \text{Null}(\mathbf{H})$, the exact Hessian matrix, \mathbf{H} , has *some* \mathbf{g} -relevant eigenvalue that is sufficiently large (in magnitude), and the gradient, \mathbf{g} , has non-trivial projection on the corresponding eigenspace. We make that assumption here as well.

Assumption 5 (Assumption 5 in [43]). *There exists $\mu > 0$ and $L_{\mathbf{g}}^2/(L_{\mathbf{g}}^2 + \eta^2) < \nu \leq 1$ such that, for any $\mathbf{x} \in \mathbb{R}^d$, if $\mathbf{g} \notin \text{Null}(\mathbf{H})$, then at least one of the following holds:*

(i) *If $\phi_+ \geq 1$ and $\phi_- \geq 1$, there exists some $1 \leq k \leq \phi_+$ and $\phi_+ + \phi_0 + 1 \leq l \leq \phi$ for which*

$$\begin{aligned} \min\{\zeta_k, |\zeta_l|\} &\geq \mu, \\ \|(\mathbf{S}_{k+}\mathbf{S}_{k+}^\top + \mathbf{S}_{l-}\mathbf{S}_{l-}^\top)\mathbf{g}\|^2 &\geq \nu\|\mathbf{S}\mathbf{S}^\top\mathbf{g}\|^2. \end{aligned}$$

(ii) *If $\phi_+ \geq 1$, there exists some $1 \leq k \leq \phi_+$, for which*

$$\begin{aligned} \zeta_k &\geq \mu, \\ \|\mathbf{S}_{k+}\mathbf{S}_{k+}^\top\mathbf{g}\|^2 &\geq \nu\|\mathbf{S}\mathbf{S}^\top\mathbf{g}\|^2. \end{aligned}$$

(iii) *If $\phi_- \geq 1$, there exists some $\phi_+ + \phi_0 + 1 \leq l \leq \phi$, for which*

$$\begin{aligned} |\zeta_l| &\geq \mu, \\ \|\mathbf{S}_{l-}\mathbf{S}_{l-}^\top\mathbf{g}\|^2 &\geq \nu\|\mathbf{S}\mathbf{S}^\top\mathbf{g}\|^2. \end{aligned}$$

Assumption 5 essentially rules out scenarios where the gradient is not entirely in the null-space of \mathbf{H} and yet it has vanishingly small projection on its range with all \mathbf{g} -relevant eigenvalues being clustered around the origin. We now investigate the consequences of Assumption 5 as they relate to the inexact Hessian, $\bar{\mathbf{H}}$, and present its result in Lemma 10. This result will allow us to derive the optimal operation complexity of Algorithm 4 under inexact Hessian.

Firstly, we introduce Lemma 9, which essentially establishes a form of Gradient-Hessian null-space regularity. More precisely, by Lemma 9, if the gradient \mathbf{g} does not lie entirely in the null-space of \mathbf{H} , the norm of its projection on the range space of \mathbf{H} constitutes a constant fraction of its total norm, uniformly in \mathbf{x} . In other words, at a given iteration, if $\mathbf{g} \notin \text{Null}(\mathbf{H})$, then \mathbf{g} cannot be arbitrarily close to being aligned with the null-space of \mathbf{H} . Such Gradient-Hessian null-space property plays a key role in the convergence analysis of earlier variants of Newton-MR in [41, 51]. However, unlike [41, 51] where such a property is assumed, here we show that it is just a consequence of Assumptions 1 and 3.

Lemma 9 (Hessian-Gradient Null-space Regularity). *Under Assumptions 1 and 3, if $\max\{\phi_+, \phi_-\} \geq 1$, then*

$$\|\mathbf{S}\mathbf{S}^\top\mathbf{g}\| \geq \left(\frac{\sigma - \varepsilon}{L_{\mathbf{g}}}\right) \|\mathbf{g}\|.$$

Proof. Note that $\mathbf{g} \in \mathcal{K}_t(\bar{\mathbf{H}}, \mathbf{g})$, and so by Assumption 3 for $t \geq 1$, we have

$$\sigma\|\mathbf{g}\|^2 \leq \langle \mathbf{g}, \bar{\mathbf{H}}\mathbf{g} \rangle \leq \langle \mathbf{g}, \mathbf{H}\mathbf{g} \rangle + \varepsilon\|\mathbf{g}\|^2.$$

Hence, $(\sigma - \varepsilon)\|\mathbf{g}\| \leq \|\mathbf{H}\mathbf{g}\|$. By the [43, Lemma 3], we get $\mathbf{H}\mathbf{y} = \mathbf{H}\mathbf{S}\mathbf{S}^\top\mathbf{y}$, for all $\mathbf{y} \in \mathcal{K}_t(\mathbf{H}, \mathbf{g})$. So it follows that

$$(\sigma - \varepsilon)\|\mathbf{g}\| \leq \|\mathbf{H}\mathbf{g}\| = \|\mathbf{H}\mathbf{S}\mathbf{S}^\top\mathbf{g}\| \leq L_{\mathbf{g}}\|\mathbf{S}\mathbf{S}^\top\mathbf{g}\|,$$

which gives the desired result. \square

To investigate the relationship between \mathbf{g} and the relevant eigenspace of $\bar{\mathbf{H}}$, we need to consider the affect of the noise model (3) on the invariant subspace of \mathbf{H} . This is adequately captured by the celebrated Davis-Kahan $\sin(\Theta)$ theorem [25, 47]. Here, we present a version of this theorem adapted to our setting.

Theorem (Davis-Kahan $\sin(\Theta)$ Theorem [25, 47]). Consider \mathbf{H} and $\bar{\mathbf{H}} = \mathbf{H} + \mathbf{E}$ with their ordered eigenvalues,

$$\rho(\mathbf{H}) = \{\tilde{\zeta}_1, \tilde{\zeta}_2, \dots, \tilde{\zeta}_{d-1}, \tilde{\zeta}_d\}, \quad \text{and} \quad \rho(\bar{\mathbf{H}}) = \{\tilde{\lambda}_1, \tilde{\lambda}_2, \dots, \tilde{\lambda}_{d-1}, \tilde{\lambda}_d\},$$

respectively. For a given $i \in \{1, 2, \dots, d\}$, let $\tilde{\mathbf{S}}_i$ and $\tilde{\mathbf{U}}_i$ be the $d \times i$ matrices whose columns are the eigenvectors corresponding to the first i^{th} eigenvalues of \mathbf{H} and $\bar{\mathbf{H}}$ respectively. For index i corresponding to positive eigenvalue, i.e. $\tilde{\lambda}_i > 0$, we have

$$\|\tilde{\mathbf{U}}_i \tilde{\mathbf{U}}_i^\top - \tilde{\mathbf{S}}_i \tilde{\mathbf{S}}_i^\top\| = \|\sin \Theta(\tilde{\mathbf{U}}_i, \tilde{\mathbf{S}}_i)\| \leq \frac{2\|\bar{\mathbf{H}} - \mathbf{H}\|}{\delta_i}$$

where $\delta_i = \tilde{\zeta}_i - \tilde{\zeta}_{i+1}$. In addition, if $i = d$, then $\delta_d = \tilde{\zeta}_{d-1} - \tilde{\zeta}_d$.

By Davis-Kahan $\sin(\Theta)$ Theorem, it is implied that for the distortion of the invariant subspaces to be bounded, the underlying spectral gap of \mathbf{H} , i.e., δ_i , must not vanish. This prompts us to make the following assumption on the spectral gap, and in turn allows us to guarantee the existence of \mathbf{g} -relevant eigenvectors/eigenvalues of $\bar{\mathbf{H}}$ within certain regions.

Assumption 6 (Spectral Gap Assumption). Consider the index $1 \leq k \leq \phi_+$ and/or $\phi_+ + \phi_0 + 1 \leq l \leq \phi$ in Assumption 5. There exists $\delta > 0$ such that

$$\delta \leq \begin{cases} \min\{\tilde{\zeta}_{\Phi(k)} - \tilde{\zeta}_{\Phi(k)+1}, \tilde{\zeta}_{\Phi(\ell)-1} - \tilde{\zeta}_{\Phi(\ell)}\}, & \text{if Assumption 5-(i) holds,} \\ \tilde{\zeta}_{\Phi(k)} - \tilde{\zeta}_{\Phi(k)+1}, & \text{if Assumption 5-(ii) holds,} \\ \tilde{\zeta}_{\Phi(\ell)-1} - \tilde{\zeta}_{\Phi(\ell)}, & \text{if Assumption 5-(iii) holds.} \end{cases}$$

Variants of such spectral gap property appear ubiquitously in the literature for symmetric eigenvalue problems [49]. Assumption 6 implies a non-vanishing gap between some \mathbf{g} -relevant eigenvalue of \mathbf{H} from Assumption 5 and its (potentially) non- \mathbf{g} -relevant neighbor.

Lemma 10. Under Assumptions 1, 3, 5 and 6, with $\varepsilon \leq \min\{\mu, \sqrt{\nu}\delta\sigma/(2(\sqrt{\nu}\delta + 4L_{\mathbf{g}}))\}$ in (3), we have at least one of the following:

(i) There exist some $1 \leq i \leq \psi_+$ and $\psi_+ + \psi_0 + 1 \leq j \leq \psi$ for which

$$\begin{aligned} \min\{\lambda_i, |\lambda_j|\} &\geq \mu - \varepsilon, \\ \|(\mathbf{U}_{i+} \mathbf{U}_{i+}^\top + \mathbf{U}_{j-} \mathbf{U}_{j-}^\top) \mathbf{g}\|^2 &\geq \frac{\nu\sigma^2}{4L_{\mathbf{g}}^2} \|\mathbf{U} \mathbf{U}^\top \mathbf{g}\|^2. \end{aligned}$$

(ii) There exists some $1 \leq i \leq \psi_+$ for which

$$\begin{aligned} \lambda_i &\geq \mu - \varepsilon, \\ \|\mathbf{U}_{i+} \mathbf{U}_{i+}^\top \mathbf{g}\|^2 &\geq \frac{\nu\sigma^2}{4L_{\mathbf{g}}^2} \|\mathbf{U} \mathbf{U}^\top \mathbf{g}\|^2. \end{aligned}$$

(iii) There exists some $\psi_+ + \psi_0 + 1 \leq j \leq \psi$ for which

$$\begin{aligned} |\lambda_j| &\geq \mu - \varepsilon, \\ \|\mathbf{U}_{j-} \mathbf{U}_{j-}^\top \mathbf{g}\|^2 &\geq \frac{\nu\sigma^2}{4L_{\mathbf{g}}^2} \|\mathbf{U} \mathbf{U}^\top \mathbf{g}\|^2. \end{aligned}$$

Proof. To spell out in details, Assumption 5-(i) implies at least one of the cases (i), (ii), or (iii); Assumption 5-(ii) implies case (ii); and Assumption 5-(iii) implies case (iii). We first establish case (ii) using Assumption 5-(ii). The reasoning for cases (i) and (iii) are similar to case (ii) with some subtle adjustments.

• **Case (ii):** To prove case (ii), we need to show the implications of Assumption 5-(ii) on the eigenvectors and eigenvalues of $\tilde{\mathbf{H}}$. Given the index $1 \leq k \leq \phi_+$ from Assumption 5-(ii), by Davis-Kahan $\sin(\Theta)$ Theorem and Assumption 6, we get

$$\frac{4\varepsilon}{\delta} \geq \frac{2\|\tilde{\mathbf{H}} - \mathbf{H}\|}{\tilde{\zeta}_{\Phi(k)} - \tilde{\zeta}_{\Phi(k)+1}} \geq \|\tilde{\mathbf{S}}_{\Phi(k)}\tilde{\mathbf{S}}_{\Phi(k)}^\top - \tilde{\mathbf{U}}_{\Phi(k)}\tilde{\mathbf{U}}_{\Phi(k)}^\top\|.$$

Note a tighter upper bound is given by $2\varepsilon/\delta$. However, to make the bounds uniform across all three cases, we choose to slightly enlarge it by a factor of two. Here, $\tilde{\mathbf{S}}_{\Phi(k)}$ consists of $\Phi(k)$ numbers of eigenvectors of \mathbf{H} , i.e., both \mathbf{g} -relevant and possibly non- \mathbf{g} -relevant ones, and $\tilde{\mathbf{U}}_{\Phi(k)}$ consists of the same number of eigenvectors of $\tilde{\mathbf{H}}$. This implies that

$$\frac{4\varepsilon}{\delta} \|\mathbf{g}\| \geq \|\tilde{\mathbf{S}}_{\Phi(k)}\tilde{\mathbf{S}}_{\Phi(k)}^\top \mathbf{g} - \tilde{\mathbf{U}}_{\Phi(k)}\tilde{\mathbf{U}}_{\Phi(k)}^\top \mathbf{g}\|.$$

By the definition of \mathbf{g} -relevant eigenvectors of \mathbf{H} , we get $\tilde{\mathbf{S}}_{\Phi(k)}\tilde{\mathbf{S}}_{\Phi(k)}^\top \mathbf{g} = \mathbf{S}_{k+}\mathbf{S}_{k+}^\top \mathbf{g}$. Hence,

$$\|\tilde{\mathbf{U}}_{\Phi(k)}\tilde{\mathbf{U}}_{\Phi(k)}^\top \mathbf{g}\| + \frac{4\varepsilon}{\delta} \|\mathbf{g}\| \geq \|\mathbf{S}_{k+}\mathbf{S}_{k+}^\top \mathbf{g}\|.$$

Next, we show that $\tilde{\mathbf{U}}_{\Phi(k)}\tilde{\mathbf{U}}_{\Phi(k)}^\top \mathbf{g} \neq \mathbf{0}$. That is, there exists at least one \mathbf{g} -relevant eigenvector in $\tilde{\mathbf{U}}_{\Phi(k)}$. For this, we just need to show that $\|\mathbf{S}_{k+}\mathbf{S}_{k+}^\top \mathbf{g}\| > 4\varepsilon\|\mathbf{g}\|/\delta$. Let's assume the opposite, that is $\|\mathbf{S}_{k+}\mathbf{S}_{k+}^\top \mathbf{g}\| - 4\varepsilon\|\mathbf{g}\|/\delta \leq 0$. In this case, we have

$$\frac{4\varepsilon}{\delta} \|\mathbf{g}\| \geq \|\mathbf{S}_{k+}\mathbf{S}_{k+}^\top \mathbf{g}\| \geq \sqrt{\nu}\|\mathbf{S}\mathbf{S}^\top \mathbf{g}\| \geq \frac{\sqrt{\nu}(\sigma - \varepsilon)}{L_{\mathbf{g}}} \|\mathbf{g}\|, \quad (5)$$

where the second and the third inequalities follow from Assumption 5-(ii) and Lemma 9, respectively. This indicates $\sqrt{\nu}\delta\sigma/(\sqrt{\nu}\delta + 4L_{\mathbf{g}}) \leq \varepsilon$, which contradicts the assumption on ε . So, we must have $\tilde{\mathbf{U}}_{\Phi(k)}\tilde{\mathbf{U}}_{\Phi(k)}^\top \mathbf{g} \neq \mathbf{0}$, i.e. there exists at least one \mathbf{g} -relevant eigenvector in $\tilde{\mathbf{U}}_{\Phi(k)}$. Hence, by Lemma 8, there exists an index, say $1 \leq i \leq \psi_+$, such that

$$\tilde{\mathbf{U}}_{\Phi(k)}\tilde{\mathbf{U}}_{\Phi(k)}^\top \mathbf{g} = \mathbf{U}_{i+}\mathbf{U}_{i+}^\top \mathbf{g},$$

which gives

$$\|\mathbf{U}_{i+}\mathbf{U}_{i+}^\top \mathbf{g}\| + \frac{4\varepsilon}{\delta} \|\mathbf{g}\| \geq \|\mathbf{S}_{k+}\mathbf{S}_{k+}^\top \mathbf{g}\|.$$

Now, using (5) again, we get

$$\|\mathbf{U}_{i+}\mathbf{U}_{i+}^\top \mathbf{g}\| \geq \left(\frac{\sqrt{\nu}(\sigma - \varepsilon)}{L_{\mathbf{g}}} - \frac{4\varepsilon}{\delta} \right) \|\mathbf{g}\|.$$

Letting $\varepsilon \leq \sqrt{\nu}\delta\sigma/(2(\sqrt{\nu}\delta + 4L_{\mathbf{g}}))$, and noting that $\|\mathbf{g}\| \geq \|\mathbf{U}\mathbf{U}^\top \mathbf{g}\|$, we have

$$\|\mathbf{U}_{i+}\mathbf{U}_{i+}^\top \mathbf{g}\|^2 \geq \frac{\nu\sigma^2}{4L_{\mathbf{g}}} \|\mathbf{U}\mathbf{U}^\top \mathbf{g}\|^2.$$

We now consider the eigenvalue. Given Assumption 5-(ii), we have $\zeta_k \geq \mu$ for some $1 \leq k \leq \phi_+$. Our aim is to show that there exists a positive \mathbf{g} -relevant eigenvalue λ of $\tilde{\mathbf{H}}$, such that $\lambda \geq \mu - \varepsilon$. In fact, the index i used in the argument above serves our requirements, i.e., we show that $\lambda_i \geq \mu - \varepsilon$. Indeed, consider the given index $1 \leq k \leq \phi_+$, its corresponding mapped index $\Phi(k)$, as well as the eigenvalues of \mathbf{H} and $\tilde{\mathbf{H}}$ up to $\Phi(k)$, respectively, as

$$\{\tilde{\zeta}_1, \tilde{\zeta}_2, \dots, \tilde{\zeta}_{\Phi(k)-1}, \tilde{\zeta}_{\Phi(k)}\}, \quad \text{and} \quad \{\tilde{\lambda}_1, \tilde{\lambda}_2, \dots, \tilde{\lambda}_{\Phi(k)-1}, \tilde{\lambda}_{\Phi(k)}\}.$$

We note that $\tilde{\zeta}_{\Phi(k)}$ is \mathbf{g} -relevant by definition of the map $\Phi(\cdot)$. However, $\tilde{\lambda}_{\Phi(k)}$ may or may not be \mathbf{g} -relevant. If $\tilde{\lambda}_{\Phi(k)}$ is \mathbf{g} -relevant, then $\tilde{\mathbf{U}}_{\Phi(k)}\tilde{\mathbf{U}}_{\Phi(k)}^\top \mathbf{g} = \mathbf{U}_{i+}\mathbf{U}_{i+}^\top \mathbf{g}$ and $\Psi(i) = \Phi(k)$. Hence, by Weyl's inequality, we know $\lambda_i = \tilde{\lambda}_{\Psi(i)} = \tilde{\lambda}_{\Phi(k)} \geq \tilde{\zeta}_{\Phi(k)} - \varepsilon$ and, by Assumption 5, $\lambda_i \geq \mu - \varepsilon$. However, if $\tilde{\lambda}_{\Phi(k)}$ is not \mathbf{g} -relevant, then we consider the preceding indices, i.e., $\Phi(k) - 1$, $\Phi(k) - 2$, and so on, until we find a \mathbf{g} -relevant eigenvalue of $\tilde{\mathbf{H}}$. By the above argument for the eigenvectors, we know that there exists at least one \mathbf{g} -relevant eigenvector in $\tilde{\mathbf{U}}_{\Phi(k)}$. The corresponding index for the \mathbf{g} -relevant eigenvalue must be the index i from that \mathbf{g} -relevant eigenvector. In this case, since $\Phi(k) > \Psi(i)$, then $\lambda_i = \tilde{\lambda}_{\Psi(i)} > \tilde{\lambda}_{\Phi(k)} \geq \tilde{\zeta}_{\Phi(k)} - \varepsilon \geq \mu - \varepsilon$.

• **Case (iii):** Similarly, for case (iii), given the index $\phi_+ + \phi_0 + 1 \leq l \leq \phi$ from Assumption 5-(iii), by Davis-Kahan sin(Θ) Theorem and Assumption 6,

$$\begin{aligned} \frac{4\varepsilon}{\delta} &\geq \frac{2\|\tilde{\mathbf{H}} - \mathbf{H}\|}{\tilde{\zeta}_{\Phi(\ell)-1} - \tilde{\zeta}_{\Phi(\ell)}} \geq \|\tilde{\mathbf{S}}_{\Phi(\ell)-1} \tilde{\mathbf{S}}_{\Phi(\ell)-1}^\top - \tilde{\mathbf{U}}_{\Phi(\ell)-1} \tilde{\mathbf{U}}_{\Phi(\ell)-1}^\top\| \\ &= \|(\mathbf{I} - \tilde{\mathbf{S}}_{\Phi(\ell)-1} \tilde{\mathbf{S}}_{\Phi(\ell)-1}^\top) - (\mathbf{I} - \tilde{\mathbf{U}}_{\Phi(\ell)-1} \tilde{\mathbf{U}}_{\Phi(\ell)-1}^\top)\|. \end{aligned}$$

The latter expression considers the eigenvectors corresponding to the negative eigenvalues from $\Phi(\ell)$ to d (with multiplicities). This in particular implies $(\mathbf{I} - \tilde{\mathbf{S}}_{\Phi(\ell)-1} \tilde{\mathbf{S}}_{\Phi(\ell)-1}^\top) \mathbf{g} = \mathbf{S}_{\ell-} \mathbf{S}_{\ell-}^\top \mathbf{g}$. With a similar reasoning as in the proof of the case (ii), we know that $(\mathbf{I} - \tilde{\mathbf{U}}_{\Phi(\ell)-1} \tilde{\mathbf{U}}_{\Phi(\ell)-1}^\top) \mathbf{g} \neq \mathbf{0}$ and, by Lemma 8, $(\mathbf{I} - \tilde{\mathbf{U}}_{\Phi(\ell)-1} \tilde{\mathbf{U}}_{\Phi(\ell)-1}^\top) \mathbf{g} = \mathbf{U}_{j-} \mathbf{U}_{j-}^\top \mathbf{g}$, for some $\psi_+ + \psi_0 + 1 \leq j \leq \psi$, which implies

$$\|\mathbf{U}_{j-} \mathbf{U}_{j-}^\top \mathbf{g}\| + \frac{4\varepsilon}{\delta} \|\mathbf{g}\| \geq \|\mathbf{S}_{\ell-} \mathbf{S}_{\ell-}^\top \mathbf{g}\|.$$

By Assumption 5-(iii), Lemma 9, and the choice of ε , we get

$$\|\mathbf{U}_{j-} \mathbf{U}_{j-}^\top \mathbf{g}\|^2 \geq \frac{\nu\sigma^2}{4L_{\mathbf{g}}} \|\mathbf{U} \mathbf{U}^\top \mathbf{g}\|^2.$$

For the eigenvalues, we consider the following two sets,

$$\{|\tilde{\zeta}_d|, |\tilde{\zeta}_{d-1}|, \dots, |\tilde{\zeta}_{\Phi(\ell)+1}|, |\tilde{\zeta}_{\Phi(\ell)}|\}, \quad \text{and} \quad \{|\tilde{\lambda}_d|, |\tilde{\lambda}_{d-1}|, \dots, |\tilde{\lambda}_{\Phi(\ell)+1}|, |\tilde{\lambda}_{\Phi(\ell)}|\}.$$

With a similar reasoning as in the proof of case (ii) and sweeping over the indices $\Phi(\ell)$, $\Phi(\ell) + 1$, etc, we get

$$|\lambda_j| \geq \mu - \varepsilon$$

where j is the index defined above in \mathbf{U}_{j-} .

• **Case (i):** Consider the indices $1 \leq k \leq \phi_+$ and $\phi_+ + \phi_0 + 1 \leq \ell \leq \phi$ given by Assumption 5-(i). Under Assumption 6, Davis-Kahan sin(Θ) Theorem gives

$$\frac{4\varepsilon}{\delta} \geq \|(\mathbf{I} - \tilde{\mathbf{S}}_{\Phi(\ell)-1} \tilde{\mathbf{S}}_{\Phi(\ell)-1}^\top) - (\mathbf{I} - \tilde{\mathbf{U}}_{\Phi(\ell)-1} \tilde{\mathbf{U}}_{\Phi(\ell)-1}^\top)\| + \|\tilde{\mathbf{S}}_{\Phi(k)} \tilde{\mathbf{S}}_{\Phi(k)}^\top - \tilde{\mathbf{U}}_{\Phi(k)} \tilde{\mathbf{U}}_{\Phi(k)}^\top\|,$$

which implies

$$\frac{4\varepsilon}{\delta} \|\mathbf{g}\| \geq \left\| \left(\tilde{\mathbf{S}}_{\Phi(k)} \tilde{\mathbf{S}}_{\Phi(k)}^\top + (\mathbf{I} - \tilde{\mathbf{S}}_{\Phi(\ell)-1} \tilde{\mathbf{S}}_{\Phi(\ell)-1}^\top) \right) \mathbf{g} - \left(\tilde{\mathbf{U}}_{\Phi(k)} \tilde{\mathbf{U}}_{\Phi(k)}^\top + (\mathbf{I} - \tilde{\mathbf{U}}_{\Phi(\ell)-1} \tilde{\mathbf{U}}_{\Phi(\ell)-1}^\top) \right) \mathbf{g} \right\|.$$

For the eigenvectors of \mathbf{H} , we have

$$(\tilde{\mathbf{S}}_{\Phi(k)} \tilde{\mathbf{S}}_{\Phi(k)}^\top + (\mathbf{I} - \tilde{\mathbf{S}}_{\Phi(\ell)-1} \tilde{\mathbf{S}}_{\Phi(\ell)-1}^\top)) \mathbf{g} = (\mathbf{S}_{k+} \mathbf{S}_{k+}^\top + \mathbf{S}_{\ell-} \mathbf{S}_{\ell-}^\top) \mathbf{g}.$$

Now, we use a similar argument as in the previous two cases. However, unlike the previous two cases, we can only guarantee

$$(\tilde{\mathbf{U}}_{\Phi(k)} \tilde{\mathbf{U}}_{\Phi(k)}^\top + (\mathbf{I} - \tilde{\mathbf{U}}_{\Phi(\ell)-1} \tilde{\mathbf{U}}_{\Phi(\ell)-1}^\top)) \mathbf{g} \neq \mathbf{0}.$$

That is, there exists at least one \mathbf{g} -relevant eigenvector in $\tilde{\mathbf{U}}_{\Phi(k)}$, $\tilde{\mathbf{U}}_{\Phi(\ell)-1}^\perp$ or both. This amounts to two scenarios. If there exists \mathbf{g} -relevant eigenvectors *only* in $\tilde{\mathbf{U}}_{\Phi(k)}$ or $\tilde{\mathbf{U}}_{\Phi(\ell)-1}^\perp$, then we are reduced to cases (ii) or (iii), i.e.,

$$(\tilde{\mathbf{U}}_{\Phi(k)} \tilde{\mathbf{U}}_{\Phi(k)}^\top + (\mathbf{I} - \tilde{\mathbf{U}}_{\Phi(\ell)-1} \tilde{\mathbf{U}}_{\Phi(\ell)-1}^\top)) \mathbf{g} = \mathbf{U}_{i+} \mathbf{U}_{i+}^\top \mathbf{g},$$

for some $1 \leq i \leq \psi_+$, or

$$(\tilde{\mathbf{U}}_{\Phi(k)} \tilde{\mathbf{U}}_{\Phi(k)}^\top + (\mathbf{I} - \tilde{\mathbf{U}}_{\Phi(\ell)-1} \tilde{\mathbf{U}}_{\Phi(\ell)-1}^\top)) \mathbf{g} = \mathbf{U}_{j-} \mathbf{U}_{j-}^\top \mathbf{g},$$

for some $\phi_+ + \phi_0 + 1 \leq j \leq \psi$, respectively. Otherwise, we must have \mathbf{g} -relevant eigenvectors in *both* $\tilde{\mathbf{U}}_{\Phi(k)}$ and $\tilde{\mathbf{U}}_{\Phi(\ell)-1}^\perp$, which by Lemma 8, implies

$$(\tilde{\mathbf{U}}_{\Phi(k)} \tilde{\mathbf{U}}_{\Phi(k)}^\top + (\mathbf{I} - \tilde{\mathbf{U}}_{\Phi(\ell)-1} \tilde{\mathbf{U}}_{\Phi(\ell)-1}^\top)) \mathbf{g} = (\mathbf{U}_{i+} \mathbf{U}_{i+}^\top + \mathbf{U}_{j-} \mathbf{U}_{j-}^\top) \mathbf{g},$$

for some $1 \leq i \leq \psi_+$ and $\phi_+ + \phi_0 + 1 \leq j \leq \psi$. In this case, we have

$$\|(\mathbf{U}_{i+}\mathbf{U}_{i+}^\top + \mathbf{U}_{j-}\mathbf{U}_{j-}^\top)\mathbf{g}\|^2 \geq \frac{\nu\sigma^2}{4L_{\mathbf{g}}}\|\mathbf{U}\mathbf{U}^\top\mathbf{g}\|^2,$$

and a similar argument as in the previous two case also gives

$$\min\{\lambda_i, |\lambda_j|\} \geq \mu - \varepsilon,$$

where i and j correspond to the indices from \mathbf{U}_{i+} and \mathbf{U}_{j-} , respectively. □

With Lemma 10 in hand, we can now use a similar strategy as [43] to obtain optimal convergence guarantees. To do that, we will first obtain upper bound estimates on the maximum iterations needed for Algorithm 1 to detect Conditions 1 and 2.

Lemma 11. *Let Assumptions 1, 3 and 6 hold and consider Assumption 5 with*

$$\frac{16L_{\mathbf{g}}^4}{(4L_{\mathbf{g}}^2 + \eta^2)\sigma^2} < \nu \leq 1,$$

where $\eta > 2L_{\mathbf{g}}\sqrt{4L_{\mathbf{g}}^2 - \sigma^2}/\sigma$. Also, suppose the noise level in (3) is small enough such that

$$\varepsilon \leq \min\left\{\frac{\sqrt{\nu}\sigma}{2(\sqrt{\nu} + 4\delta L_{\mathbf{g}})}, \frac{\mu}{2}\right\}.$$

- If $\psi_- \geq 1$, after at most

$$T_N \triangleq \min\left\{\max\left\{\left\lceil\left(\frac{\sqrt{2(L_{\mathbf{g}} + \mu)/\mu}}{4}\right)\log\left[\frac{2(L_{\mathbf{g}} + \mu)(4L_{\mathbf{g}}^2 - \nu\sigma^2)}{\mu\nu\sigma^2}\right] + 1\right\rceil, 1\right\}, d\right\}$$

iterations, the NPC Condition 2 will be detected.

- If $\psi_+ \geq 1$, after at most

$$T_S \triangleq \min\left\{\left\lceil\frac{\sqrt{L_{\mathbf{g}}/\mu}}{2}\log\left[4\left/\left(\frac{\eta^2}{4L_{\mathbf{g}}^2 + \eta^2} - \left(1 - \frac{\nu\sigma^2}{4L_{\mathbf{g}}^2}\right)\right)\right] + 1\right\rceil, d\right\}$$

iterations, the inexactness Condition 1 will be satisfied.

Proof. The bounds are simple consequences of [43, Corollaries 1 and 2] using constants adapted to the case of inexact Hessian. Specifically, we first recall that by Assumption 1, we have $\lambda_1 \leq L_{\mathbf{g}} + \varepsilon$.

- Suppose $\psi_- \geq 1$ and let j be the index given in Lemma 10 for which we have $|\lambda_j| \geq \mu - \varepsilon$. Applying [43, Corollary 2], coupled with Lemma 10 and $\varepsilon \leq \mu/2$ gives the bound on T_N .

- Now suppose $\psi_+ \geq 1$. By Lemma 10, there is some $1 \leq i \leq \psi_+$ for which $\lambda_i \geq \mu - \varepsilon$. From [43, Corollary 1], for this i , we obtain

$$T_S \geq \frac{\sqrt{\lambda_1/\lambda_i}}{4}\log\left(4\left/\left(\frac{\eta^2}{\|\mathbf{U}^\top\bar{\mathbf{H}}\mathbf{U}\|^2 + \eta^2} - \frac{\|(\mathbf{U}\mathbf{U}^\top - \mathbf{U}_{i+}\mathbf{U}_{i+}^\top)\mathbf{g}\|^2}{\|\mathbf{U}_{i+}\mathbf{U}_{i+}^\top\mathbf{g}\|^2}\right)\right)\right).$$

By Lemma 10,

$$\frac{\|(\mathbf{U}\mathbf{U}^\top - \mathbf{U}_{i+}\mathbf{U}_{i+}^\top)\mathbf{g}\|^2}{\|\mathbf{U}_{i+}\mathbf{U}_{i+}^\top\mathbf{g}\|^2} \geq 1 - \frac{\nu\sigma^2}{4L_{\mathbf{g}}^2}$$

and, with $L_{\mathbf{g}} \geq \varepsilon$,

$$4L_{\mathbf{g}}^2 \geq (L_{\mathbf{g}} + \varepsilon)^2 \geq (\|\mathbf{U}^\top\mathbf{E}\mathbf{U}\| + \|\mathbf{U}^\top\mathbf{H}\mathbf{U}\|)^2 \geq \|\mathbf{U}^\top\bar{\mathbf{H}}\mathbf{U}\|^2,$$

which using $\varepsilon \leq \mu/2$ gives the desired bound. □

We now obtain the optimal operation complexity of Algorithm 4. The proof is almost identical to [43, Theorem 4], and hence is omitted.

Theorem 3 (Optimal Operation Complexity of Algorithm 4). *Suppose d is sufficiently large. Under Assumptions 1 to 6, with ε in (3) satisfying*

$$\varepsilon \leq \min \left\{ \frac{\sqrt{\varepsilon_{\mathbf{g}}}}{\eta + \sigma}, \frac{\sigma(1 - 2\rho_S)}{2}, 1 - \rho_N, \frac{\sqrt{\nu}\sigma}{2(\sqrt{\nu} + 4\delta L_{\mathbf{g}})}, \frac{\mu}{2} \right\},$$

after at most $\tilde{O}(\varepsilon_{\mathbf{g}}^{-3/2})$ gradient and Hessian-vector product evaluations, Algorithm 4 satisfies the approximated first-order optimality (2a). Here, ρ_N and ρ_S are the line-search parameters from Algorithm 4.

3.2.2 Second-order Complexity

To achieve second-order optimality (2), in addition to verifying $\|\mathbf{g}_k\| \leq \varepsilon_{\mathbf{g}}$, one also needs to check for the minimum eigenvalue of \mathbf{H}_k . Similarly to the case where the exact Hessian is used [43, Section 3.3], here we can also rely on Algorithm 1 and its inherent ability to provide a certificate of positive semi-definiteness for $\bar{\mathbf{H}}$. For this, when $\|\mathbf{g}_k\| \leq \varepsilon_{\mathbf{g}}$, we run Algorithm 1 with $\bar{\mathbf{H}}_k + 0.5(\varepsilon_{\mathbf{H}} - \varepsilon)\mathbf{I}_d$ and $\tilde{\mathbf{g}}$, where $\tilde{\mathbf{g}}$ is generated from a uniform distribution on the unit sphere. This way, $\tilde{\mathbf{g}}$ will have non-trivial projection on all eigenspaces associated with $\bar{\mathbf{H}}$, with probability one. In other words, the grade of $\tilde{\mathbf{g}}$ with respect to $\bar{\mathbf{H}}$ is, almost surely, the same as the number of distinct eigenvalues of $\bar{\mathbf{H}}$. As a result, with probability one, $\bar{\mathbf{H}}_k + 0.5(\varepsilon_{\mathbf{H}} - \varepsilon)\mathbf{I}_d \not\leq \mathbf{0}$ if and only if Algorithm 1 detects a NPC direction.

If, after certain number of iterations (see Lemma 12), the NPC Condition 2 has not been detected, then we must have $\lambda_{\min}(\bar{\mathbf{H}}) \geq -(\varepsilon_{\mathbf{H}} - \varepsilon)$, which by Weyl's inequality implies $\lambda_{\min}(\mathbf{H}_k) \geq -\varepsilon_{\mathbf{H}}$, i.e., second-order optimality (2) is achieved. Otherwise, when Condition 2 is detected, we have

$$\left\langle \mathbf{r}_k^{(t-1)}, \bar{\mathbf{H}}_k \mathbf{r}_k^{(t-1)} \right\rangle \leq -\frac{(\varepsilon_{\mathbf{H}} - \varepsilon)}{2} \left\| \mathbf{r}_k^{(t-1)} \right\|^2.$$

We set $\mathbf{d}_k = -\text{Sign}(\langle \mathbf{g}_k, \mathbf{r}_k^{(t-1)} \rangle) \mathbf{r}_k^{(t-1)} / \|\mathbf{r}_k^{(t-1)}\|$ and use

$$f(\mathbf{x}_k + \alpha_k \mathbf{d}_k) \leq f(\mathbf{x}_k) + \frac{1}{2} \rho_N \alpha_k^2 \langle \mathbf{d}_k, \bar{\mathbf{H}}_k \mathbf{d}_k \rangle, \quad (6)$$

with $0 < \rho_N < 1$, as our line-search (see Algorithm 5).

Second-order Iteration Complexity

By leveraging the results of Section 3.2.1, to obtain iteration complexity for Algorithm 5, we just need to consider the main additional step in Line 12 where we either obtain a direction of nonpositive curvature or a certificate of approximate second-order optimality. Lemma 12 gives a bound for decrease in f in case of the former.

Lemma 12. *Suppose Assumption 2 holds and consider (3) with $\varepsilon \leq \varepsilon_{\mathbf{H}} \min\{(1 - \rho_N)/(2(3 - \rho_N)), 1/10\}$. Further, suppose $\lambda_{\min}(\bar{\mathbf{H}}) \leq -\varepsilon_{\mathbf{H}} + \varepsilon$ and Step 12 of Algorithm 5 returns an NPC direction. We have*

$$f(\mathbf{x}_{k+1}) - f(\mathbf{x}_k) \leq -c_4 \varepsilon_{\mathbf{H}}^3,$$

where

$$c_4 \triangleq \frac{9\rho_N(3 - \rho_N)^2}{4(4L_{\mathbf{H}})^2},$$

and ρ_N is the curvature parameter of the line-search (6).

Proof. We can clearly write

$$\begin{aligned} \langle \mathbf{d}_k, \mathbf{H}_k \mathbf{d}_k \rangle &= \langle \mathbf{d}_k, \bar{\mathbf{H}}_k \mathbf{d}_k \rangle - \langle \mathbf{d}_k, \mathbf{E}_k \mathbf{d}_k \rangle \\ &= \left\langle \mathbf{d}_k, \left(\bar{\mathbf{H}}_k + \frac{\varepsilon_{\mathbf{H}} - \varepsilon}{2} \mathbf{I} \right) \mathbf{d}_k \right\rangle - \frac{\varepsilon_{\mathbf{H}} - \varepsilon}{2} \|\mathbf{d}_k\|^2 - \langle \mathbf{d}_k, \mathbf{E}_k \mathbf{d}_k \rangle \end{aligned}$$

Note that $\|\mathbf{d}_k\| = 1$, and since $\text{Type} = \text{NPC}$, the first term is nonpositive. Hence,

$$\langle \mathbf{d}_k, \mathbf{H}_k \mathbf{d}_k \rangle \leq -\frac{(\varepsilon_{\mathbf{H}} - \varepsilon)}{2} - \langle \mathbf{d}_k, \mathbf{E}_k \mathbf{d}_k \rangle \leq -\frac{(\varepsilon_{\mathbf{H}} - \varepsilon)}{2} + \varepsilon = \frac{3\varepsilon - \varepsilon_{\mathbf{H}}}{2}.$$

Algorithm 5 Newton-MR with Second-Order Complexity Guarantee with Inexact Hessian

Require:

- Initial point: \mathbf{x}_0
- First-order and second-order optimality tolerance: $0 < \varepsilon_{\mathbf{g}} \leq 1$ and $0 < \varepsilon_{\mathbf{H}} \leq 1$
- Sub-problem Inexactness tolerance : $\eta > 0$

```
1: Let  $k = 0$ 
2: while True do
3:   if  $\|\mathbf{g}_k\| > \varepsilon_{\mathbf{g}}$  then
4:     Call MINRES Algorithm 1:  $(\mathbf{d}_k, \text{Type}) = \text{MINRES}(\bar{\mathbf{H}}_k, \mathbf{g}_k, \eta)$ 
5:     if Type = SOL then
6:       Use Algorithm 2 to obtain  $\alpha_k$  satisfying (4) with  $\rho = \rho_S$  where  $0 < \rho_S < 1/2$ .
7:     else
8:       Use Algorithm 3 to obtain  $\alpha_k$  satisfying (4) with  $\rho = \rho_N$  where  $0 < \rho_N < 1$ .
9:     end if
10:  else
11:    Randomly generate a vector  $\tilde{\mathbf{g}}$  from a uniform distribution on a unit sphere.
12:    Call MINRES Algorithm 1:  $(\mathbf{d}_k, \text{Type}) = \text{MINRES}(\bar{\mathbf{H}}_k + 0.5(\varepsilon_{\mathbf{H}} - \varepsilon)\mathbf{I}_d, \tilde{\mathbf{g}}, 0)$ 
13:    if Type = 'SOL' then
14:      Terminate
15:    else
16:      Set  $\mathbf{d}_k = -\text{Sign}(\langle \mathbf{g}_k, \mathbf{d}_k \rangle) \mathbf{d}_k / \|\mathbf{d}_k\|$  (NB: "Sign(0)" can be arbitrarily chosen as " $\pm 1$ ")
17:      Use Algorithm 3 to obtain  $\alpha_k$  satisfying (6) with  $0 < \rho_N < 1$ .
18:    end if
19:  end if
20:   $\mathbf{x}_{k+1} = \mathbf{x}_k + \alpha_k \mathbf{d}_k$ 
21:   $k = k + 1$ 
22: end while
23: return  $\mathbf{x}_k$ 
```

We also have $\langle \mathbf{d}_k, \mathbf{g}_k \rangle < 0$, which using Assumption 2 implies

$$\begin{aligned} f(\mathbf{x}_{k+1}) - f(\mathbf{x}_k) &\leq \alpha_k \langle \mathbf{d}_k, \mathbf{g}_k \rangle + \frac{\alpha_k^2}{2} \langle \mathbf{d}_k, \mathbf{H}_k \mathbf{d}_k \rangle + \frac{L_{\mathbf{H}}}{6} \alpha_k^3 \|\mathbf{d}_k\|^3 \\ &\leq \frac{\alpha_k^2}{2} \langle \mathbf{d}_k, \mathbf{H}_k \mathbf{d}_k \rangle + \frac{L_{\mathbf{H}}}{6} \alpha_k^3 \|\mathbf{d}_k\|^3. \end{aligned}$$

Also, $\langle \mathbf{d}_k, \mathbf{H}_k \mathbf{d}_k \rangle - \varepsilon \leq \langle \mathbf{d}_k, \bar{\mathbf{H}} \mathbf{d}_k \rangle$. Putting them together, the line-search is satisfied if for some $0 < \alpha \leq 1$ we have,

$$\frac{\alpha_k^2}{2} \langle \mathbf{d}_k, \mathbf{H}_k \mathbf{d}_k \rangle + \frac{L_{\mathbf{H}}}{6} \alpha_k^3 \|\mathbf{d}_k\|^3 \leq \frac{1}{2} \rho_N \alpha_k^2 \langle \mathbf{d}_k, \mathbf{H}_k \mathbf{d}_k \rangle - \frac{\rho_N \alpha_k^2}{2} \varepsilon,$$

which implies

$$\alpha_k \leq \frac{3(1 - \rho_N) \varepsilon_{\mathbf{H}} - 3(3 - \rho_N) \varepsilon}{2L_{\mathbf{H}}}.$$

With $\varepsilon \leq (1 - \rho_N) \varepsilon_{\mathbf{H}} / (2(3 - \rho_N))$, it follows that for the step size accepted by the line-search (6), we must have

$$\alpha_k \geq \frac{3(3 - \rho_N) \varepsilon_{\mathbf{H}}}{4L_{\mathbf{H}}}.$$

So, by the choice of ε , we have $\varepsilon \leq \varepsilon_{\mathbf{H}}/5$. Hence, it follows that

$$\begin{aligned} f(\mathbf{x}_{k+1}) - f(\mathbf{x}_k) &\leq \frac{1}{2} \rho_N \alpha_k^2 \langle \mathbf{d}_k, \bar{\mathbf{H}} \mathbf{d}_k \rangle \leq \frac{1}{2} \rho_N \alpha_k^2 \langle \mathbf{d}_k, \mathbf{H}_k \mathbf{d}_k \rangle + \frac{1}{2} \rho_N \alpha_k^2 \varepsilon \\ &\leq \frac{\rho_N \alpha_k^2 (3\varepsilon - \varepsilon_{\mathbf{H}})}{4} + \frac{1}{2} \rho_N \alpha_k^2 \varepsilon = \frac{\rho_N (5\varepsilon - \varepsilon_{\mathbf{H}}) \alpha_k^2}{4} \\ &\leq \frac{-\rho_N (\varepsilon_{\mathbf{H}} - 5\varepsilon)}{4} \left(\frac{3(3 - \rho_N) \varepsilon_{\mathbf{H}}}{4L_{\mathbf{H}}} \right)^2, \end{aligned}$$

which implies the desired result using $\varepsilon \leq \varepsilon_{\mathbf{H}}/10$. \square

Putting all of the previous results together, we can provide the optimal iteration complexity of Algorithm 5 for obtaining a point satisfying the approximate second-order optimality (2). Proof is similar to [43, Theorem 5], and hence is omitted.

Theorem 4 (Second-Order Optimal Iteration Complexity of Newton-MR). *Under Assumptions 1 to 4, with $\eta = \theta \sqrt{\varepsilon_{\mathbf{g}}}$ for some $\theta > 0$ in Condition 1, and ε in (3) satisfying*

$$\varepsilon \leq \min \left\{ \frac{\sqrt{\varepsilon_{\mathbf{g}}}}{\eta + \sigma}, \frac{\sigma(1 - 2\rho_S)}{2}, 1 - \rho_N, \frac{\varepsilon_{\mathbf{H}}}{10}, \frac{(1 - \rho_N) \varepsilon_{\mathbf{H}}}{2(3 - \rho_N)} \right\},$$

after at most

$$K \triangleq \left\lceil \frac{2(f(\mathbf{x}_0) - f^*)}{\min\{2c_1, 2c_2, 2c_3, c_4\}} \max\{\varepsilon_{\mathbf{g}}^{-3/2}, \varepsilon_{\mathbf{H}}^{-3}\} + 1 \right\rceil,$$

iterations of Algorithm 5, the approximate second-order optimality (2) is satisfied with probability one. Here c_1, c_2, c_3 , and c_4 are defined in Lemmas 4 to 6 and 12, ρ_N and ρ_S are the line-search parameters from Algorithm 5, and $f^* \triangleq \min f(\mathbf{x})$.

Second-order Operation Complexity

To provide an operation complexity for Algorithm 5, we can leverage the results of Section 3.2.1. What is left is to obtain the complexity of performing Step 12 of Algorithm 5. By [53, Lemma 9] or [36, Theorem 4.2], with a probability of at least $1 - p$, after at most,

$$t \geq \min \left\{ \left\lceil \left(\frac{1}{4\sqrt{\varepsilon_{\mathbf{M}}}} \right) \log \left[\frac{2.75d}{p^2} \right] + 1 \right\rceil, d \right\},$$

iterations, we have

$$\lambda_{\min}(\tilde{\mathbf{T}}_t) - \lambda_{\min}(\bar{\mathbf{H}} + 0.5(\varepsilon_{\mathbf{H}} - \varepsilon)\mathbf{I}) \leq \varepsilon_{\mathbf{M}} \left(\lambda_{\max}(\bar{\mathbf{H}} + 0.5(\varepsilon_{\mathbf{H}} - \varepsilon)\mathbf{I}) - \lambda_{\min}(\bar{\mathbf{H}} + 0.5(\varepsilon_{\mathbf{H}} - \varepsilon)\mathbf{I}) \right),$$

where $\tilde{\mathbf{T}}_t$ is the tridiagonal matrix obtained from $\bar{\mathbf{H}} + 0.5(\varepsilon_{\mathbf{H}} - \varepsilon)\mathbf{I}$. With $\varepsilon_{\mathbf{M}} = (\varepsilon_{\mathbf{H}} - \varepsilon)/(8L_{\mathbf{g}})$,

$$\begin{aligned} \lambda_{\min}(\tilde{\mathbf{T}}_t) - \lambda_{\min}(\bar{\mathbf{H}} + 0.5(\varepsilon_{\mathbf{H}} - \varepsilon)\mathbf{I}) &\leq \frac{\varepsilon_{\mathbf{H}} - \varepsilon}{8L_{\mathbf{g}}} (\lambda_{\max}(\bar{\mathbf{H}} + 0.5(\varepsilon_{\mathbf{H}} - \varepsilon)\mathbf{I}) - \lambda_{\min}(\bar{\mathbf{H}} + 0.5(\varepsilon_{\mathbf{H}} - \varepsilon)\mathbf{I})) \\ &\leq \frac{\varepsilon_{\mathbf{H}} - \varepsilon}{8L_{\mathbf{g}}} (\lambda_{\max}(\bar{\mathbf{H}}) - \lambda_{\min}(\bar{\mathbf{H}})) \\ &\leq \frac{\varepsilon_{\mathbf{H}} - \varepsilon}{8L_{\mathbf{g}}} (L_{\mathbf{g}} + \varepsilon + L_{\mathbf{g}} + \varepsilon) \leq \frac{\varepsilon_{\mathbf{H}} - \varepsilon}{2}. \end{aligned}$$

Hence,

$$\lambda_{\min}(\bar{\mathbf{H}}) \geq \lambda_{\min}(\tilde{\mathbf{T}}_t) - \varepsilon_{\mathbf{H}} + \varepsilon.$$

Consequently, with $\varepsilon \leq \varepsilon_{\mathbf{H}}/2$, if after at most

$$T_L \triangleq \min \left\{ \left\lceil \left(\sqrt{\frac{L_{\mathbf{g}}}{\varepsilon_{\mathbf{H}}}} \log \left[\frac{2.75d}{p^2} \right] + 1 \right) \right\rceil, d \right\},$$

iterations, Condition 2 is not triggered, then we must have $\lambda_{\min}(\tilde{\mathbf{T}}_t) > 0$ with probability $1 - p$. Now, [42, Theorem 3.3], implies second-order optimality condition, i.e., $\lambda_{\min}(\bar{\mathbf{H}}) \geq -\varepsilon_{\mathbf{H}} + \varepsilon$.

Theorem 5 (Second-Order Operation Complexity of Newton-MR). *Suppose d is sufficiently large. Under Assumptions 1 to 6, with ε in (3) satisfying*

$$\varepsilon \leq \min \left\{ \frac{\sqrt{\varepsilon_{\mathbf{g}}}}{\eta + \sigma}, \frac{\sigma(1 - 2\rho_S)}{2}, 1 - \rho_N, \frac{\varepsilon_{\mathbf{H}}}{10}, \frac{(1 - \rho_N)\varepsilon_{\mathbf{H}}}{2(3 - \rho_N)} \right\},$$

after at most $\max \left\{ \tilde{\mathcal{O}}(\varepsilon_{\mathbf{g}}^{-3/2}), \tilde{\mathcal{O}}(\varepsilon_{\mathbf{H}}^{-7/2}) \right\}$ gradient and Hessian-vector product evaluations, Algorithm 5 satisfies the approximated second-order optimality (2) with high probability. Here, ρ_N and ρ_S are the line-search parameters from Algorithm 5.

4 Numerical Experiments

For our numerical experiments, we consider a series of finite-sum minimization problems. We evaluate the performance of Algorithm 4 in comparison with several other second-order methods, namely Newton-CG [53] and its sub-sampled variant [66], Steihaug's trust-region method [23, 46] and its corresponding sub-sampled algorithms [62, 65, 66], as well as L-BFGS [46]. We approximate the Hessian by means of sub-sampling, e.g. 5% or 10% of the total samples. For each experiment, the performance is depicted in two plots, namely the graph of $f(\mathbf{x})$ with respect to the number of iterations as well as a corresponding plot based on the number of function oracle calls. For instance, the amount of work required for computing the gradient can be considered as equivalent to two oracle calls, i.e., one forward and one backward propagation, and a Hessian-vector product operation can be obtained through a work equivalent to four oracle calls (see [41, 51] for more details).

Implementation details

For the line-search Algorithms 2 and 3 in Algorithm 4, the parameters are set to $\rho_N = \rho_S = 10^{-4}$. Similarly, in Newton-CG, the Armijo line-search parameters is also set to 10^{-4} . For L-BFGS, the limited memory size is set to 20, and the Armijo and the Strong Wolfe line-search parameters are, respectively, set to their typical values of 10^{-4} and 0.9. For trust-region method, following the notation used in [23], the parameters η_1 and η_2 are set to 1/4 and 3/4 respectively. The selection of the inexactness parameter η in Newton-MR is aimed at enabling the algorithm to generate directions of `Type = SOL` as frequently as feasible. Similarly, we adopt a comparable approach when determining the inexactness tolerance for Capped-CG, as well as the damping parameter ξ , represented by $\tilde{\mathbf{H}} = \bar{\mathbf{H}} + \xi\mathbf{I}$ in the context of Newton-CG. Hence, these parameters are set to different values across the following

experiments. For Sections 4.2 and 4.3, all algorithms are terminated when either the oracle calls reach 10^6 , the magnitude of the gradient falls below 10^{-8} , or the step size/trust region goes below 10^{-18} . As such, our first-order sub-optimality is set to $\varepsilon_{\mathbf{g}} = 10^{-8}$.

In the legends of Figures 3 and 4, ‘ $x\%$ ’ and ‘Single Sample’ refer to when the approximate Hessian is formed using an ‘ x ’ percent of the full dataset and one single sample, respectively. For all other figures, ‘algorithm_hsub- x ’ refers to a given algorithm when $100x$ percent of the full dataset is used to construct the Hessian. When there is no postfix, the Hessian matrix is formed exactly.

4.1 Binary Classification

We first investigate the advantages/disadvantages of Hessian approximation within Newton-MR framework using two simple finite-sum problems in the form of binary classification. Namely, we consider convex binary logistic regression (Figure 4),

$$f(\mathbf{x}) = \frac{1}{n} \sum_{i=1}^n \ln(1 + \exp(\langle \mathbf{a}_i, \mathbf{x} \rangle)) - b_i \langle \mathbf{a}_i, \mathbf{x} \rangle,$$

and nonconvex non-linear least square (Figure 3),

$$f(\mathbf{x}) = \frac{1}{n} \left(\sum_{i=1}^n \frac{1}{1 + \exp(-\langle \mathbf{a}_i, \mathbf{x} \rangle)} - b_i \right)^2.$$

For our experiments here, we use the MNIST data set [26], which contains of 60,000 grayscale images of size 28×28 , i.e., $\{(\mathbf{a}_i, b_i)\}_{i=1}^{n=60,000} \subset \mathbb{R}^{784} \times [0, 1]$. The labels of MNIST dataset are converted to binary classification, i.e. even and odd numbers.

In Algorithm 4, we set $\eta = 0.01$ and $\mathbf{x}_0 = \mathbf{0}$. The results of running Algorithm 4 using various degrees of Hessian approximation are given in Figures 3 and 4. As it can be seen, while Hessian approximation generally helps with reducing the overall computational costs, its effectiveness can diminish if the approximation is overly crude. This is expected since a significant reduction in sub-sample size could lead to substantial loss of curvature information, resulting in poor performance.

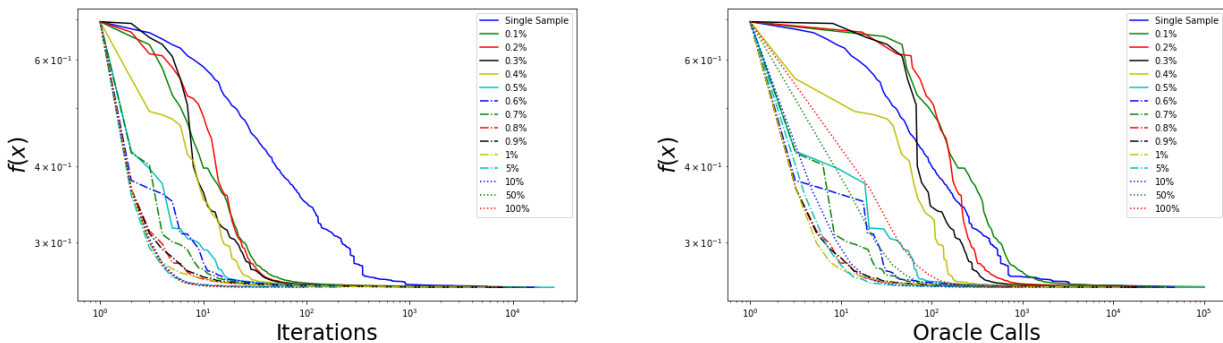


Figure 3: Performance of Algorithm 4 using various degrees of Hessian approximation on the convex logistic loss function. Single sample refers the case when the Hessian is formed with only one sample. As it can be seen, Hessian approximation typically reduces computational costs; however, a substantial reduction in sub-sample size can lead to significant loss of curvature information, resulting in poorer performance.

4.2 Feed Forward Neural Network

In this section, we consider a multi-class classification problem using a feed forward neural network, namely

$$f(\mathbf{x}) = -\frac{1}{n} \left(\sum_{i=1}^n \langle \mathbf{b}_i, \ln(\mathbf{h}(\mathbf{x}; \mathbf{a}_i)) \rangle \right) + \lambda g(\mathbf{x}), \quad (7)$$

where $\mathbf{h}(\mathbf{x}; \mathbf{a}_i) : \mathbb{R}^d \rightarrow [0, 1]^C$ represent the output of the neural network, $\mathbf{b}_i \in \{0, 1\}^C$ denotes the labels corresponding to input data \mathbf{a}_i , $g(\mathbf{x}) : \mathbb{R}^d \rightarrow \mathbb{R}$ is a nonconvex regularizer defined as $g(\mathbf{x}) \triangleq \sum_{i=1}^d x_i^2 / (1 + x_i^2)$, and $\lambda > 0$ is a regularization parameter.

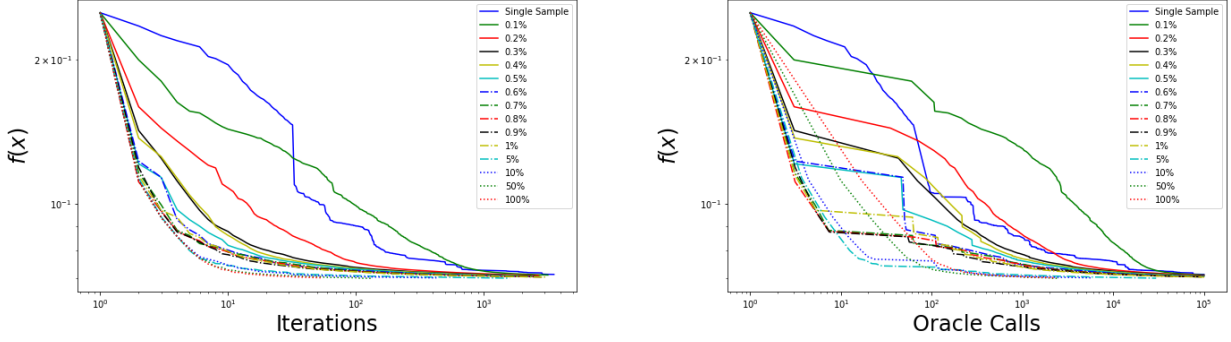


Figure 4: Performance of Algorithm 4 using various degrees of Hessian approximation on the nonconvex non-linear least squares loss function. Single sample refers the case when the Hessian is formed with only one sample. As it can be seen, Hessian approximation typically reduces computational costs; however, a substantial reduction in sub-sample size can lead to significant loss of curvature information, resulting in poorer performance.

For the experiments in Figures 5 to 7, we use CIFAR10 dataset [35], consisting of 60,000 colored images of size 32×32 in 10 classes, i.e., $\{(\mathbf{a}_i, \mathbf{b}_i)\}_{i=1}^{n=6,000} \subset \mathbb{R}^{3,072} \times \{0, 1\}^{10}$. The feed forward neural network has the following architecture,

$$3072 \text{ (input)} \rightarrow \tanh \rightarrow 512 \rightarrow \tanh \rightarrow 256 \rightarrow \tanh \rightarrow 128 \rightarrow \text{softmax} \rightarrow 10 \text{ (output)},$$

resulting in $d = 1,738,890$ numbers of parameters. The regularization parameter is set to $\lambda = 10^{-8}$. All algorithms are initialized from a normal distribution with zero mean and co-variance $0.1\mathbf{I}$. The inexactness parameter of Algorithm 4 is set to $\eta = 10$. For Newton-CG [53, 66], the desired accuracy for Capped-CG is set to 0.9, the damping parameter is set to $\xi = 0.9$.

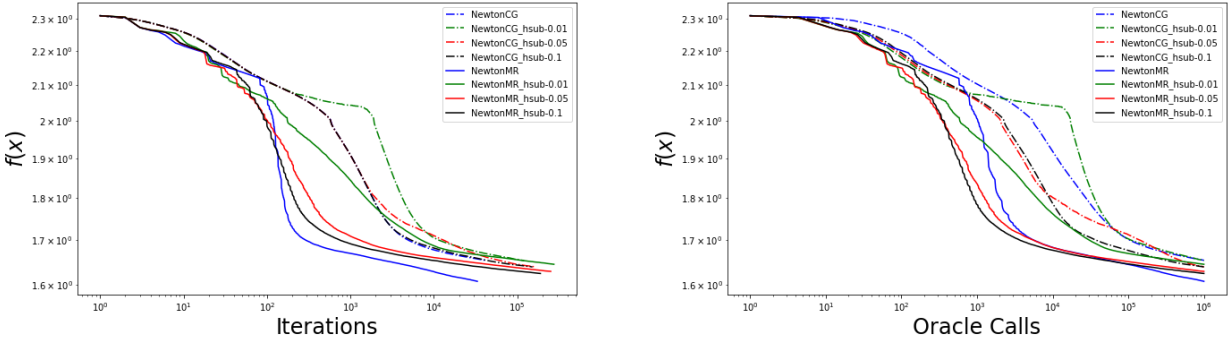


Figure 5: Comparison of Newton-MR and Newton-CG on CIFAR10 dataset in Section 4.2.

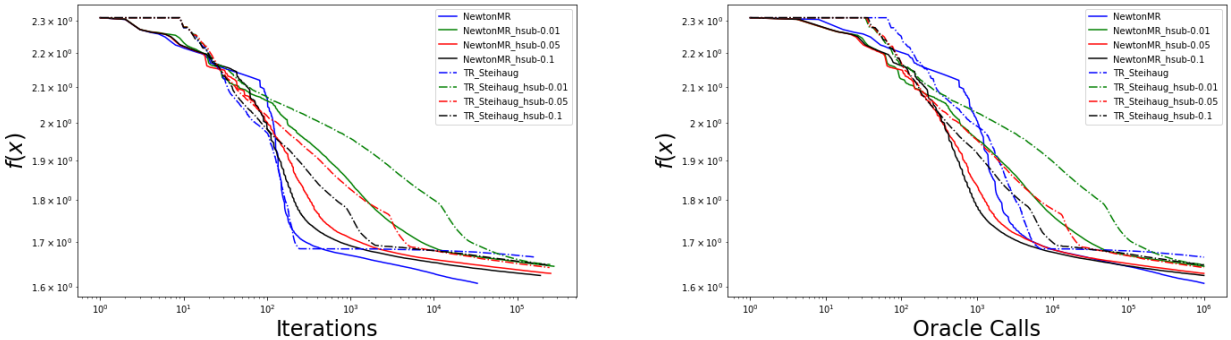


Figure 6: Comparison of Newton-MR and Trust-Region on CIFAR10 dataset in Section 4.2.

Next, we consider a different dataset, namely Coverttype [12], which includes $n = 581,012$ samples of 54 attributes across seven classes. For the experiments involving this dataset, the neural network

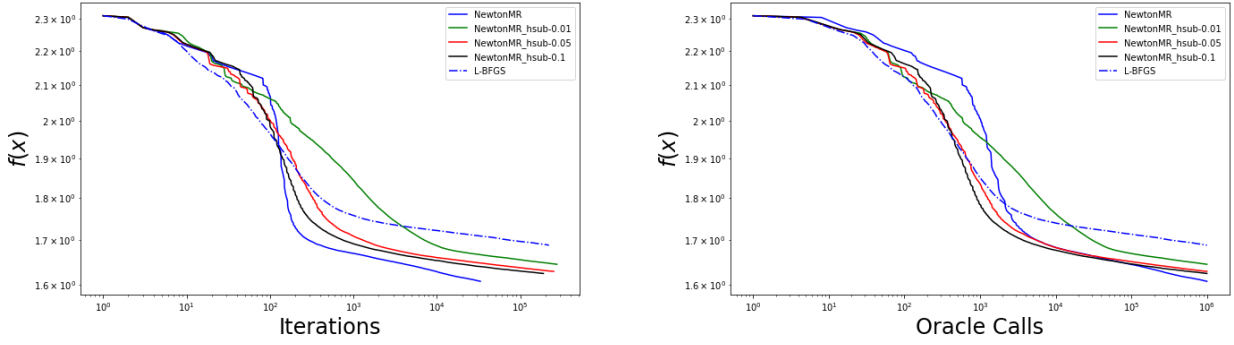


Figure 7: Comparison of Newton-MR and L-BFGS on CIFAR10 dataset in Section 4.2.

architecture is chosen to be

$$54 \text{ (input)} \rightarrow \tanh \rightarrow 512 \rightarrow \tanh \rightarrow 256 \rightarrow \text{softmax} \rightarrow 7 \text{ (output)},$$

resulting in $d = 161,287$. We also set $\lambda = 10^{-8}$. Again, \mathbf{x}_0 is chosen as above. For Newton-MR, the sub-problem inexactness parameter is changed to $\eta = 10,000$. For Newton-CG, the desired accuracy and the Hessian regularization parameter are both set to 0.99. The underlying parameters of the L-BFGS and trust-region methods also remain the same as above. The results are depicted in Figures 8 to 10.

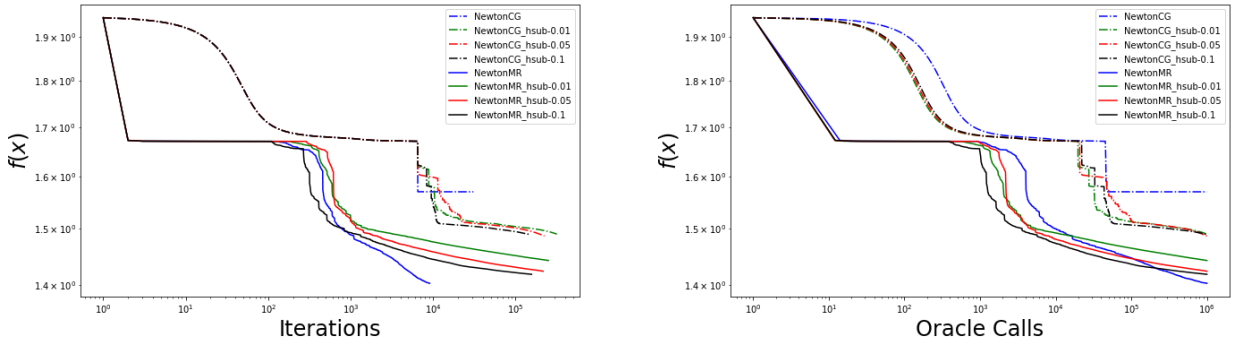


Figure 8: Comparison of Newton-MR and Newton-CG on Covertypes dataset for training a feed forward network as in Section 4.2.

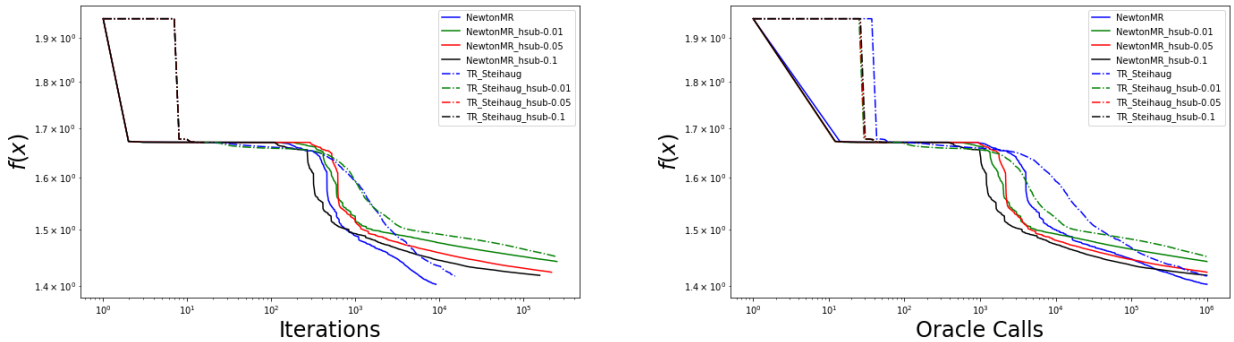


Figure 9: Comparison of Newton-MR and Trust-Region on Covertypes dataset for training a feed forward network as in Section 4.2.

In all Figures 5 to 10, Algorithm 4 with appropriate degree of sub-sampling either is very competitive with, or downright superior to, all other methods that we have considered. What is striking is the relative poor performance of all Newton-CG variants. This further corroborates the observations in [41, 43, 51] that MINRES typically manifests itself as a far superior inner solver than the widely

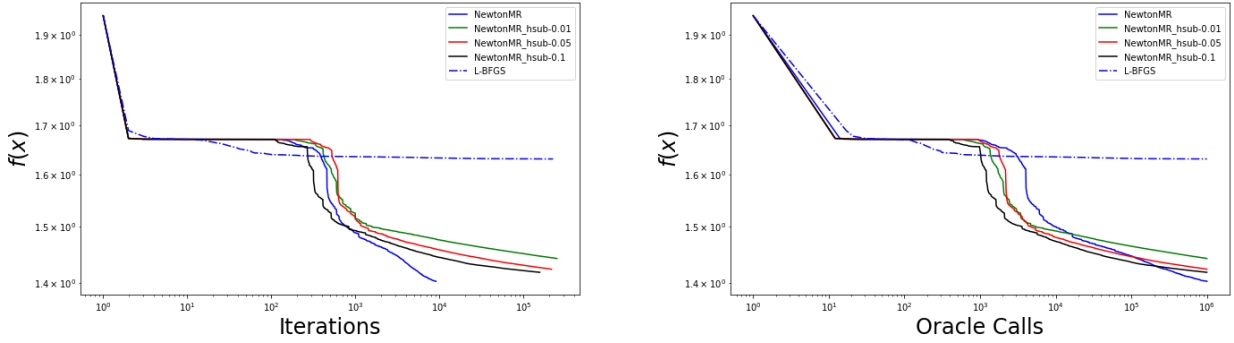


Figure 10: Comparison of Newton-MR and L-BFGS on Covertypes dataset for training a feed forward network as in Section 4.2.

used CG method. Note that, in Figure 9, both TR_Steihaug_hsub-0.05 and TR_Steihaug_hsub-0.1 are terminated in about 80 iterations, as their trust regions shrink to 10^{-26} radius.

4.3 Recurrent Neural Network

Finally, we consider a slightly more challenging problem of training a recurrent neural network (RNN) [58] with mean squared error loss. Specifically, we consider the following objective function

$$f(\mathbf{x}) = \frac{1}{n} \sum_{i=1}^n \|\mathbf{h}(\mathbf{x}; \mathbf{a}_i) - \mathbf{b}_i\|^2 + \lambda g(\mathbf{x}),$$

where $\mathbf{h}(\mathbf{x}; \mathbf{a})$ is the output of the RNN and $g(\mathbf{x})$ is again the same nonconvex regularizer as in Section 4.2 with regularization parameter $\lambda = 0.1$.

For the experiment here, we use the Gas sensor array under dynamic gas mixtures data set [28], which is a time series data. In particular, the data contains a time series of 16 features across two time stamps. So, we get $\{\mathbf{a}_i, \mathbf{b}_i\}_{i=1}^{n=137,485} \subset (\mathbb{R}^2 \times \mathbb{R}^{16}) \times \mathbb{R}^{16}$, and $d = 138,640$. All algorithms are initialized from a normal distribution with zero mean and co-variance $10^{-8}\mathbf{I}$. For Newton-MR, the relative residual tolerance is set to $\eta = 10$. For Newton-CG, the desired accuracy and the damping parameter are both set to 0.99.

The results are given in Figures 11 to 13. Once again, in all these experiments, Algorithm 4 with adequate sub-sampling can either outperform or at least remain competitive with the alternative methods. Also, one can again observe the visibly poor performance of Newton-CG relative to Algorithm 4. In Figure 13, L-BFGS is terminated in about 2000 iterations, as its step size gets below 10^{-18} .

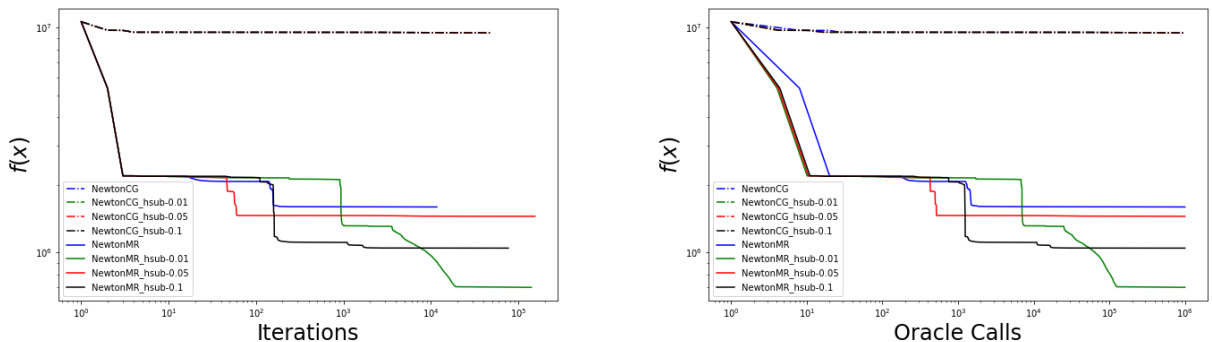


Figure 11: Comparison of Newton-MR and Newton-CG for training a recurrent neural network as in Section 4.3.

5 Conclusion

We considered variants of the Newton-MR algorithm for nonconvex problems, initially proposed in [43], where the Hessian matrix is suitable approximated. We first considered a special class of nonconvex

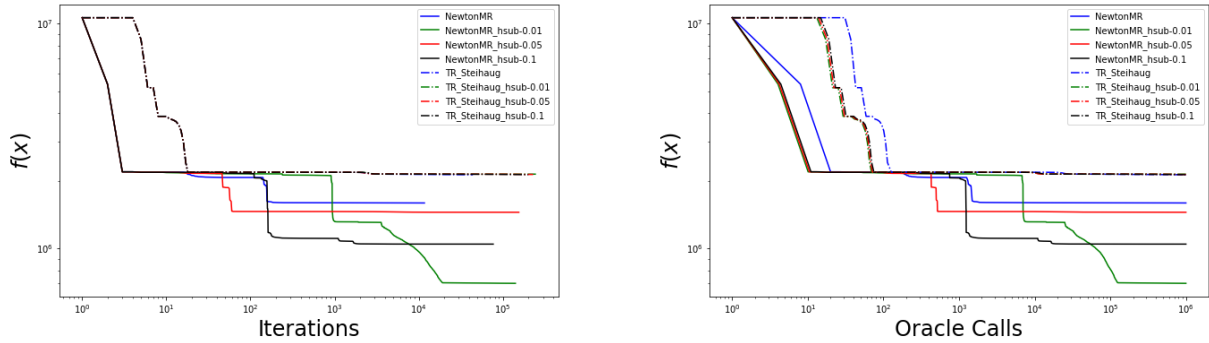


Figure 12: Comparison of Newton-MR and Trust-Region for training a recurrent neural network as in Section 4.3.

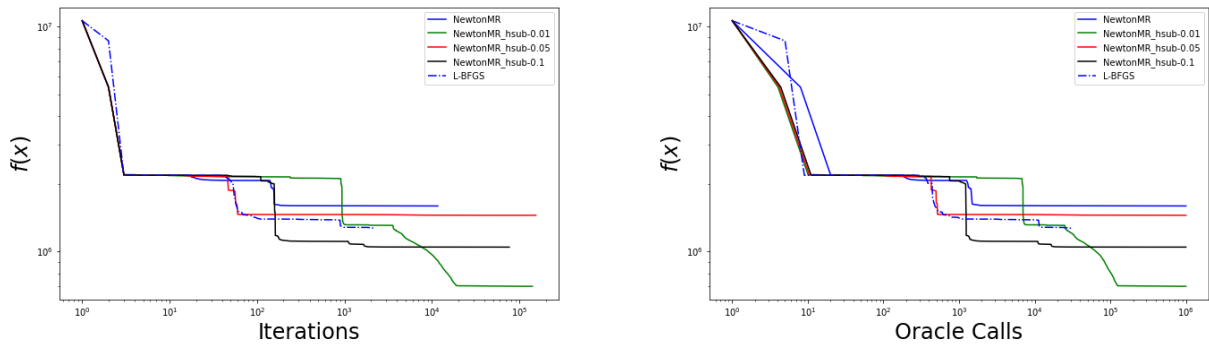


Figure 13: Comparison of Newton-MR and L-BFGS for training a recurrent neural network as in Section 4.3.

functions, namely those satisfying the Polyak-Lojasiewicz property. In such settings, we showed that under rather mild conditions, our algorithms converge with a linear rate. In particular, the linear convergence rate is obtained regardless of the degree of approximation of the Hessian as well as the accuracy of the solution to the sub-problem.

We then considered more general nonconvex settings and showed that our variants maintain similar convergence guarantees as their exact counterparts. While establishing iteration complexity proved to be rather straightforward extension from [43], obtaining the state-of-the-art operation complexity involved a much finer grained analysis to study the effect of our additive noise model on the eigenvalues and eigenvectors of the inexact Hessian. Finally we provided numerical experiments on several machine learning problem to further illustrate the advantages of sub-sampled Hessian in the Newton-MR framework.

5.1 Acknowledgments

Fred Roosta was partially supported by the Australian Research Council through an Industrial Transformation Training Centre for Information Resilience (IC200100022) as well as a Discovery Early Career Researcher Award (DE180100923).

References

- [1] Motasem Alfarra, Slavomir Hanzely, Alyazeed Albasyoni, Bernard Ghanem, and Peter Richtárik. Adaptive learning of the optimal batch size of sgd. *arXiv preprint arXiv:2005.01097*, 2020.
- [2] A. Beck. *First-Order Methods in Optimization*. MOS-SIAM Series on Optimization. Society for Industrial and Applied Mathematics, 2017.

- [3] Stefania Bellavia, Eugenio Fabrizi, and Benedetta Morini. Linesearch newton-cg methods for convex optimization with noise. *ANNALI DELL'UNIVERSITA' DI FERRARA*, 68(2):483–504, 2022.
- [4] Stefania Bellavia and Gianmarco Gurioli. Stochastic analysis of an adaptive cubic regularization method under inexact gradient evaluations and dynamic Hessian accuracy. *Optimization*, 71(1):227–261, 2022.
- [5] Stefania Bellavia, Gianmarco Gurioli, and Benedetta Morini. Adaptive cubic regularization methods with dynamic inexact Hessian information and applications to finite-sum minimization. *IMA Journal of Numerical Analysis*, 41(1):764–799, 2021.
- [6] Stefania Bellavia, Gianmarco Gurioli, Benedetta Morini, and Ph L Toint. Trust-region algorithms: Probabilistic complexity and intrinsic noise with applications to subsampling techniques. *EURO Journal on Computational Optimization*, 10:100043, 2022.
- [7] Stefania Bellavia, Gianmarco Gurioli, Benedetta Morini, and Philippe L Toint. Quadratic and Cubic Regularisation Methods with Inexact function and Random Derivatives for Finite-Sum Minimisation. In *2021 21st International Conference on Computational Science and Its Applications (ICCSA)*, pages 258–267. IEEE, 2021.
- [8] Stefania Bellavia, Nataša Krejić, and Nataša Krklec Jerinkić. Subsampled inexact newton methods for minimizing large sums of convex functions. *IMA Journal of Numerical Analysis*, 40(4):2309–2341, 2020.
- [9] Stefania Bellavia, Nataša Krejić, and Benedetta Morini. Inexact restoration with subsampled trust-region methods for finite-sum minimization. *Computational Optimization and Applications*, 76:701–736, 2020.
- [10] Albert S Berahas, Raghu Bollapragada, and Jorge Nocedal. An investigation of newton-sketch and subsampled newton methods. *Optimization Methods and Software*, 35(4):661–680, 2020.
- [11] El Houcine Bergou, Youssef Diouane, Vladimir Kunc, Vyacheslav Kungurtsev, and Clément W Royer. A subsampling line-search method with second-order results. *INFORMS Journal on Optimization*, 4(4):403–425, 2022.
- [12] Jock Blackard. Covertypes. UCI Machine Learning Repository, 1998. DOI: <https://doi.org/10.24432/C50K5N>.
- [13] Jose Blanchet, Coralia Cartis, Matt Menickelly, and Katya Scheinberg. Convergence rate analysis of a stochastic trust-region method via supermartingales. *INFORMS journal on optimization*, 1(2):92–119, 2019.
- [14] Raghu Bollapragada, Richard H Byrd, and Jorge Nocedal. Exact and inexact subsampled Newton methods for optimization. *IMA Journal of Numerical Analysis*, 39(2):545–578, 2019.
- [15] Richard H. Byrd, Gillian M. Chin, Will Neveitt, and Jorge Nocedal. On the use of stochastic Hessian information in optimization methods for machine learning. *SIAM Journal on Optimization*, 21(3):977–995, 2011.
- [16] Richard H. Byrd, Gillian M. Chin, Jorge Nocedal, and Yuchen Wu. Sample size selection in optimization methods for machine learning. *Mathematical programming*, 134(1):127–155, 2012.
- [17] Coralia Cartis, Nicholas IM Gould, and Ph L Toint. Complexity bounds for second-order optimality in unconstrained optimization. *Journal of Complexity*, 28(1):93–108, 2012.
- [18] Coralia Cartis, Nicholas IM Gould, and Philippe L Toint. Adaptive cubic regularisation methods for unconstrained optimization. part i: motivation, convergence and numerical results. *Mathematical Programming*, 127(2):245–295, 2011.
- [19] Coralia Cartis, Nicholas IM Gould, and Philippe L Toint. Adaptive cubic regularisation methods for unconstrained optimization. part ii: worst-case function-and derivative-evaluation complexity. *Mathematical programming*, 130(2):295–319, 2011.

- [20] Coralia Cartis, Nicholas IM Gould, and Philippe L Toint. *Evaluation Complexity of Algorithms for Nonconvex Optimization: Theory, Computation and Perspectives*. SIAM, 2022.
- [21] Coralia Cartis and Katya Scheinberg. Global convergence rate analysis of unconstrained optimization methods based on probabilistic models. *Mathematical Programming*, 169:337–375, 2018.
- [22] Ruobing Chen, Matt Menickelly, and Katya Scheinberg. Stochastic optimization using a trust-region method and random models. *Mathematical Programming*, 169:447–487, 2018.
- [23] Andrew R Conn, Nicholas IM Gould, and Philippe L Toint. *Trust region methods*. SIAM, 2000.
- [24] Marie-Ange Dahito and Dominique Orban. The Conjugate Residual Method in Linesearch and Trust-Region Methods. *SIAM Journal on Optimization*, 29(3):1988–2025, 2019.
- [25] Chandler Davis and William Morton Kahan. The rotation of eigenvectors by a perturbation. iii. *SIAM Journal on Numerical Analysis*, 7(1):1–46, 1970.
- [26] Li Deng. The mnist database of handwritten digit images for machine learning research [best of the web]. *IEEE signal processing magazine*, 29(6):141–142, 2012.
- [27] Murat A Erdogdu and Andrea Montanari. Convergence rates of sub-sampled newton methods. *Advances in Neural Information Processing Systems*, 28, 2015.
- [28] Jordi Fonollosa, Sadique Sheik, Ramón Huerta, and Santiago Marco. Reservoir computing compensates slow response of chemosensor arrays exposed to fast varying gas concentrations in continuous monitoring. *Sensors and Actuators B: Chemical*, 215:618–629, 2015.
- [29] Ian Goodfellow, Yoshua Bengio, and Aaron Courville. *Deep learning*. MIT press, 2016.
- [30] Robert Gower, Dmitry Kovalev, Felix Lieder, and Peter Richtárik. Rsn: Randomized subspace newton. *Advances in Neural Information Processing Systems*, 32, 2019.
- [31] Serge Gratton, Sadok Jerad, and Philippe Toint. First-order objective-function-free optimization algorithms and their complexity. *arXiv preprint arXiv:2203.01757*, 2022.
- [32] Serge Gratton, Sadok Jerad, and Philippe Toint. Complexity of a class of first-order objective-function-free optimization algorithms. *arXiv preprint arXiv:2203.01647*, 2023.
- [33] Serge Gratton, Clément W Royer, Luís N Vicente, and Zaikun Zhang. Complexity and global rates of trust-region methods based on probabilistic models. *IMA Journal of Numerical Analysis*, 38(3):1579–1597, 2018.
- [34] Serge Gratton and Philippe Toint. Offo minimization algorithms for second-order optimality and their complexity. *Computational Optimization and Applications*, 84(2):573–607, 2023.
- [35] Alex Krizhevsky, Geoffrey Hinton, et al. Learning multiple layers of features from tiny images. 2009.
- [36] Jacek Kuczyński and Henryk Woźniakowski. Estimating the largest eigenvalue by the power and lanczos algorithms with a random start. *SIAM journal on matrix analysis and applications*, 13(4):1094–1122, 1992.
- [37] G. Lan. *First-order and Stochastic Optimization Methods for Machine Learning*. Springer Series in the Data Sciences. Springer International Publishing, 2020.
- [38] Jeffrey Larson and Stephen C Billups. Stochastic derivative-free optimization using a trust region framework. *Computational Optimization and applications*, 64:619–645, 2016.
- [39] Z. Lin, H. Li, and C. Fang. *Accelerated Optimization for Machine Learning: First-Order Algorithms*. Springer Singapore, 2020.
- [40] Dong C Liu and Jorge Nocedal. On the limited memory bfgs method for large scale optimization. *Mathematical programming*, 45(1-3):503–528, 1989.

- [41] Yang Liu and Fred Roosta. Convergence of newton-mr under inexact hessian information. *SIAM Journal on Optimization*, 31(1):59–90, 2021.
- [42] Yang Liu and Fred Roosta. Minres: From negative curvature detection to monotonicity properties. *SIAM Journal on Optimization*, 32(4):2636–2661, 2022.
- [43] Yang Liu and Fred Roosta. A newton-mr algorithm with complexity guarantees for nonconvex smooth unconstrained optimization. *arXiv preprint arXiv:2208.07095*, 2022.
- [44] Shashi K Mishra and Giorgio Giorgi. *Invecity and optimization*, volume 88. Springer Science & Business Media, 2008.
- [45] Yurii Nesterov and Boris T Polyak. Cubic regularization of Newton method and its global performance. *Mathematical Programming*, 108(1):177–205, 2006.
- [46] Jorge Nocedal and Stephen Wright. *Numerical optimization*. Springer Science & Business Media, 2006.
- [47] Sean O’Rourke, Van Vu, and Ke Wang. Random perturbation of low rank matrices: Improving classical bounds. *Linear Algebra and its Applications*, 540:26–59, 2018.
- [48] Christopher C Paige and Michael A Saunders. Solution of sparse indefinite systems of linear equations. *SIAM journal on numerical analysis*, 12(4):617–629, 1975.
- [49] Beresford N. Parlett. *The Symmetric Eigenvalue Problem*. Society for Industrial and Applied Mathematics, 1998.
- [50] Mert Pilanci and Martin J Wainwright. Newton sketch: A near linear-time optimization algorithm with linear-quadratic convergence. *SIAM Journal on Optimization*, 27(1):205–245, 2017.
- [51] Fred Roosta, Yang Liu, Peng Xu, and Michael W Mahoney. Newton-mr: Inexact newton method with minimum residual sub-problem solver. *EURO Journal on Computational Optimization*, 10:100035, 2022.
- [52] Farbod Roosta-Khorasani and Michael W Mahoney. Sub-sampled newton methods. *Mathematical Programming*, 174(1):293–326, 2019.
- [53] Clément W Royer, Michael O’Neill, and Stephen J Wright. A newton-cg algorithm with complexity guarantees for smooth unconstrained optimization. *Mathematical Programming*, 180:451–488, 2020.
- [54] Clément W Royer and Stephen J Wright. Complexity analysis of second-order line-search algorithms for smooth nonconvex optimization. *SIAM Journal on Optimization*, 28(2):1448–1477, 2018.
- [55] Sebastian Ruder. An overview of gradient descent optimization algorithms. *arXiv preprint arXiv:1609.04747*, 2016.
- [56] Shai Shalev-Shwartz and Shai Ben-David. *Understanding machine learning: From theory to algorithms*. Cambridge university press, 2014.
- [57] Sara Shashaani, Fatemeh S Hashemi, and Raghu Pasupathy. Astro-df: A class of adaptive sampling trust-region algorithms for derivative-free stochastic optimization. *SIAM Journal on Optimization*, 28(4):3145–3176, 2018.
- [58] Alex Sherstinsky. Fundamentals of recurrent neural network (rnn) and long short-term memory (lstm) network. *Physica D: Nonlinear Phenomena*, 404:132306, 2020.
- [59] Yingjie Tian, Yuqi Zhang, and Haibin Zhang. Recent advances in stochastic gradient descent in deep learning. *Mathematics*, 11(3):682, 2023.
- [60] Nilesh Tripuraneni, Mitchell Stern, Chi Jin, Jeffrey Regier, and Michael I Jordan. Stochastic cubic regularization for fast nonconvex optimization. *Advances in neural information processing systems*, 31, 2018.

- [61] Stephen J Wright and Benjamin Recht. *Optimization for data analysis*. Cambridge University Press, 2022.
- [62] Peng Xu, Fred Roosta, and Michael W Mahoney. Newton-type methods for non-convex optimization under inexact hessian information. *Mathematical Programming*, 184(1-2):35–70, 2020.
- [63] Peng Xu, Fred Roosta, and Michael W Mahoney. Second-order optimization for non-convex machine learning: An empirical study. In *Proceedings of the 2020 SIAM International Conference on Data Mining*, pages 199–207. SIAM, 2020.
- [64] Peng Xu, Jiyang Yang, Fred Roosta, Christopher Ré, and Michael W Mahoney. Sub-sampled Newton methods with non-uniform sampling. In *Advances in Neural Information Processing Systems (NeurIPS-16)*, pages 3000–3008, 2016.
- [65] Zhewei Yao, Peng Xu, Fred Roosta, and Michael W Mahoney. Inexact nonconvex Newton-type methods. *INFORMS Journal on Optimization*, 3(2):154–182, 2021.
- [66] Zhewei Yao, Peng Xu, Fred Roosta, Stephen J Wright, and Michael W Mahoney. Inexact Newton-CG algorithms with complexity guarantees. *IMA Journal of Numerical Analysis*, 43(3):1855–1897, 2023.
- [67] Ya-xiang Yuan. A review of trust region algorithms for optimization. In *Iciam*, volume 99, pages 271–282, 2000.
- [68] Ya-xiang Yuan. Recent advances in trust region algorithms. *Mathematical Programming*, 151:249–281, 2015.